APPLICATION OF SMART MATERIAL ON THE OVERTOPPING TYPE WAVE ENERGY CONVERTER

A Thesis

by

CHIA-HUNG CHIEN

Submitted to the Office of Graduate and Professional Studies of
Texas A&M University
in partial fulfillment of the requirements for the degree of

MASTER OF SCIENCE

Chair of Committee,	Kuang-An Chang
Committee Members,	James M. Kaihatu
	Jun Kameoka
Head of Department,	Sharath Girimaji

December 2017

Major Subject: Ocean Engineering

ABSTRACT

This thesis presents a method of applying “Shape Memory Alloy” (SMA) on an overtopping wave energy converter (OWEC). A control system which can fit all sea states is necessary for OWEC to adapt to a mutative wave condition and achieve an optimal overtopping discharge rate. Among all the parameters affecting the overtopping discharge rate, the crest freeboard height is the most influential one. To change the crest freeboard height, commonly used old methods include installation of a hinge at the bottom and adjustment of the floating height of the entire device. Both of them will inevitably affect other parameters while changing the crest freeboard height. To fill this gap, the application of SMA springs, which can solely adjust the crest freeboard height, will benefit the optimization of the OWECs.

In a laboratory test, a scaled down physical model is placed in a water tank. The entire model is set to be fixed in the water tank and there are two boards, which are connected by the SMA springs, represent as a ramp that waves need to overcome. The SMA springs are able to change their length by the temperature change. A LabVIEW program sent spectra-wave signals to the wave maker and a pumping system is used to calculate the mean overtopping discharge rate.

The result of non-using SMA springs follows the rule of the overtopping discharge rate. But, there are some differences with the general formula of the OWEC which comes from the different experimental setups and the limitation of the water tank. However, this

result is useful to become the reference of the result of using SMA springs which shows that there is no significant change at the mean overtopping discharge rate and the errors are acceptable. All of the results and comparisons indicate that the concept of applying the SMA springs on the OWEC is proven.

ACKNOWLEDGEMENTS

I would like to thank my committee chair, Dr. Chang, and my committee members, Dr. Kaihatu and Dr. Kameoka, for their guidance and support throughout the course of this research and countless discussions and suggestions so that I can finish this research.

I also would like to thank Amy Pan, Wei-Liang Chuang, Sina Baghbani Kordmahale, and Jonnie Reed, thanks to all for their help and time spent in teaching me how to improve my research. Thanks also go to my friends, who spent their time to have joy with me in this two years, and the department faculty and staff for making my time at Texas A&M University a great experience.

Finally, thanks to my family for their mental encouragement and financial support. Without them, I cannot have this wonderful experience in my life.

CONTRIBUTORS AND FUNDING SOURCES

Contributors

Graduate study was partially supported by a funding from the “Development of Synergetic/mobile Multi-source Multi-purpose Ocean Renewable Energy Station” project from TAMU Energy Institute. This work was supported by a thesis committee consisting of Professor Kuang-An Chang and Professor James M. Kaihatu of the Department of Ocean Engineering and Professor Jun Kameoka of the Department of Electrical & Computer Engineering.

All work for the thesis was completed independently by the student.

Funding Sources

Graduate study was partially supported by a funding from the “Development of Synergetic/mobile Multi-source Multi-purpose Ocean Renewable Energy Station” project from TAMU Energy Institute.

NOMENCLATURE

ξ_{p0}	Breaker Parameter
R_c	Crest Freeboard Height
a	Coefficient of Dimensionless Overtopping Discharge Equation
b	Coefficient of Dimensionless Overtopping Discharge Equation
λ_s	Correction Coefficient of Crest Freeboard Height
λ_{dr}	Correction Coefficient of Draft
λ_α	Correction Coefficient of Slope Angle
ρ	Density of Water
q_{Spill}	Discharge from Spilling Out
$q_{Turbine}$	Discharge pass through the Turbine
h	Distance between MWL in Reservoir and Bottom of Reservoir
h_t	Distance between MWL in Reservoir and SWL
h_R	Distance between the Crest Freeboard and Bottom of Reservoir
Q	Dimensionless Overtopping Discharge
R	Dimensionless Crest Freeboard Height
d_r	Draft
η_{fc}	Efficiency of Frequency Converters
η_{hyd}	Efficiency of Hydraulic Power
η_{PMG}	Efficiency of Generator
η_{turb}	Efficiency of Turbine

EIA	Energy Information Administration
g	Gravity Acceleration
GHG	Greenhouse Gas
q	Mean Overtopping Discharge
MWL	Mean Water Level
α_m	Optimal Slope Angle
OB	Oscillating Body
OWC	Oscillating Water Column
OWEC	Overtopping Wave Energy Converter
T_p	Peak Period
P_{crest}	Potential Energy of Overtopping Wave
P_{hyd}	Potential Energy in Reservoir
P_{act}	Power Delivered to the Grid
P_{est}	Power Produced by Turbine
PTO	Power Take Off
PLC	Programmable Logic Controller
α	Ramp Slope
γ	Reduction Coefficient
SMA	Shape-Memory Alloy
SMM	Shape-Memory Material
H_{m0}	Significant Wave Height
H_s	Significant Wave Height

WD	Wave Dragon
WEC	Wave Energy Converter
WG	Wave Gauge
k_p	Wave Number based on Peak Period
d	Water Depth

TABLE OF CONTENTS

Page

LIST OF FIGURES

Page

LIST OF TABLES

Page

1. INTRODUCTION

1.1 Background and Motivation

1.1.1 Renewable Energy

Due to the awakening of the environmental awareness and the limited amount of the fossil fuel, oil, and gas and their environmental footprints, the development and utilization of renewable energy sources have become more and more popular and important. By the middle of 21st century, the renewable energy sources can account for 60% of the worldwide electricity [1].

The non-renewable energy such as burning the coal, natural gas, and oil causes the carbon dioxide, a dominant type of greenhouse gas (GHG), enters the atmosphere. Indeed, the energy generation accounts for approximately 70% of all anthropogenic GHG emission [2]. The growing emission of the carbon dioxide not only deteriorates the quality of the atmosphere but also changes the climate. There is more and more evidence show that the climate change is directly related to the emission of the carbon dioxide due to human activities [3]. As more and more GHG is discharged, the temperature will increase and make the global warming worse.

Using the renewable energy is one of the promising ways to solve these problems. For now, the renewable energy cannot entirely replace the non-renewable energy due to their higher costs and lower converting efficiencies. According to the data of the U.S Energy Information Administration (EIA), in 2016, most of the U.S. electricity was generated by using the fossil fuels. In the total of 4 trillion kilowatt-hours of electricity

generated, 30% and 34% was contributed by the coals and the natural gas, respectively. Renewable energy sources only provide 15% of the U.S electricity [4]. Figure 1 shows the source of the U.S. electricity generation in 2016. Currently, wind, solar, biomass, geothermal, and hydro power generations are called as renewable energy. They are often investigated as alternative methods to supply sufficient energy in the future.

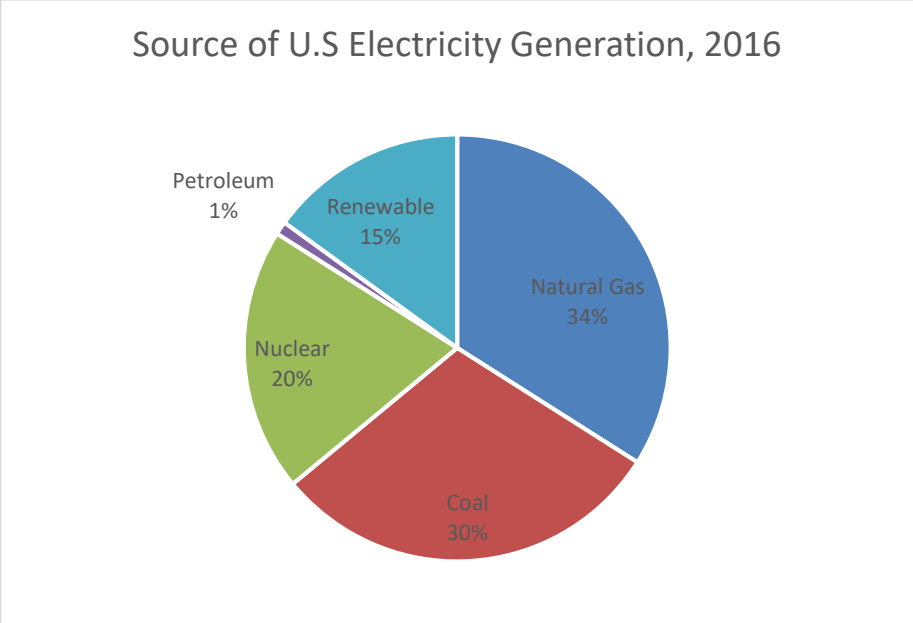

Figure 1. Source of U.S Electricity Generation reprinted from [4]

Wind power, one of the most mature renewable energy, provided almost 6% of the U.S. electricity generation. Greenpeace indicates that the wind energy will supply about 10% electricity by the year 2020. For decades, the wind has been used to mechanically rotate turbines in wind power generators and produce electricity [5]. However, the number of locations where strong winds continuously blow all year round is highly limited.

Solar power is also a widely used renewable energy. It is derived directly from the energy of the sun. Solar power systems have some advantages over traditional methods such as that they don't produce any air pollution or noise and have fewer influences to the environment [6]. However, they still have some limitations. For example, the amount of sunlight variation depends on some reasons such as the location, the time of a day, the season of a year, and the weather conditions.

Biomass is one of the earliest energy sources. Compared with other renewable technologies such as wind or solar, biomass has fewer problems with energy storage. The energy contained in biomass originally comes from the sun. Carbon dioxide in the air is transformed into other carbon-containing molecules in plants through photosynthesis process [7]. However, the biomass energy still has some environmental issues such as releasing mercury fly ash into the air during the combustion [8].

Geothermal power comes from continuous heat energy buried under the surface of the earth. The hot water or steam is converted to electrical energy via turbine generators [9].

Hydro power holds an important status in the renewable energy. It is one of the oldest and biggest renewable energy sources for the electricity generation in the U.S. Although the percentage of other types of renewable energy continuously grow, the hydropower generation systems still account for 45% of all the renewable electricity generation in 2016. There are several kinds of hydro power generation systems: the dam, the tidal power, the ocean thermal energy, and the wave power. The most common one is the dam with hydroelectric generators. Even though the dam doesn't produce too many

pollutants, the resulting reservoir might cause the change of the eco-system in impacting the fish migration, natural water temperature, water chemistry, river flow characteristics, and silt load [10].

Tidal power and ocean thermal conversion energy are also being used as hydro power. A two-way tidal power system generates electricity from both incoming and outgoing tides. The disadvantages of the tidal power are that a tidal range of 10 feet is needed to produce tidal energy economically and the eco-system at the tidal basin will be affected. There is no tidal power plant in the U.S. because only a little of them can generate power economically [11]. Ocean thermal energy conversion is based on the temperature difference. Due to the challenge of the technology, there is no large-scale operation of the ocean thermal energy conversion exists nowadays [12].

1.1.2 Wave Energy

A kind of powerful and unlimited hydro power hasn't attracted attention from the public which is the "Wave Energy". Wave energy is the most promising hydro power since 70% of the earth surface is covered by the ocean. Ocean wave contains tremendous energy. According to the data of EIA, the potential energy of waves is much more than the other hydro power resources. The ocean wave energy is estimated from 1.59 to 2.64 trillion kilowatt-hours per year. It is equal to 65% of the U.S. electricity generation in 2016 and the west coasts of the U.S. are potential sites for developing the wave energy technologies [13].

There are many approaches to convert the wave power into usable energy for the human. All of these approaches are in large-scales to generate powers, but the efficiencies

are lower and the costs are higher when comparing to the traditional power sources. Many projects are investigating to harness the power more efficiently. The objective of this thesis is to apply an innovative technology which is called “Smart Material” on a selected wave energy converter (WEC) and make the material changes its property to adjust to different wave states properly. With this new type of design, more wave power can be captured from the ocean.

1.2 Types of Wave Energy Converter

There are several kinds of WEC have been used in the past. All of them can roughly be classified into three major types: Oscillating Body, Oscillating Water Column, and Overtopping Wave Energy Converter [14].

Oscillating Body (OB) devices oscillate and the relative motion between the bodies and the seabed or between the bodies themselves are used to drive the Power Take Off (PTO) systems. They often used in deep-water regions which have more powerful waves. Generally, the PTO systems are the issue in this type of WEC because they make the whole converting system more complicated. The OBs are advantageous in possessing small sizes and floating devices, making them very versatile [15].

Oscillating Water Column (OWC) can be divided into two types, fixed and floating structures. The main concept of the OWCs is that the free sea surface will oscillate in the chamber to push the air go through the turbine to rotate. For fixed structures, the devices need to be fixed to the seabed, resulting most of them located on the shoreline or near shore. This kind of near shore structures have the advantages of easy installation and

maintenance and do not require mooring systems but in the trade-off of the lack of powerful waves. For the floating structures, most of them are operating in the deep-water regions and using slack-moored systems which are largely free to oscillate. If the OWCs are designed properly, the wave energy absorption can be enhanced [16].

Overtopping Wave Energy Converter (OWEC) is closely related to the discharge of the waves overtop the device and the amount of the water that can be stored in a reservoir at the back of the structure. If water can be heavily captured at the proper wave states and the water level in the reservoir is higher than the sea water level (SWL), draining all the water out through the turbines at the bottom of the reservoir will convert the potential energy to the electricity [16]. The main advantage of the OWECs is their simplicity, i.e., they store the water and when the water level in the reservoir is high enough, let the water pass through the turbines [15]. Table 1 lists some of the power production of several WECs that have been used in the past.

Device	Power per Unit (kW)	Depth (m)	Size
Oceantec	500	30~50	medium
Pelamis	750	50~70	medium
P P Converter	3620	Deep	large
Seabased	15	30~50	small
Wave Dragon	7000	30~50	large
Aqua Buoy	250	>50	small
AWS	2320	40~100	medium
Langlee	1665	Deep	medium
OE Buoy	2800	Deep	medium
Wavebob	1000	Deep	medium

Table 1. Comparison of Some Basic Characteristics of the Devices reprinted from [17]

1.3 Wave Dragon

The simplicity of the OWECs would enable possible alterations in parameters to fulfill the objective of the research to refine the existing setups. There are three kinds of OWECs. The most classic and the oldest one is a floating device called “Wave Dragon (WD)”. Figure 2 shows the simple design of the WD which consists of a big platform as a reservoir, several turbines at the bottom of the reservoir, and two reflectors to collect waves from a wider range of directional waves, reflecting the waves toward the platform and focusing them in front of the ramp to make more waves overtop. A 1:4.5 scale

prototype has been tested at Nissum Bredning, a large inland waterway in Denmark. Based on the data during the operating time, the converting efficiency, the ratio of the average electric power generated by the operating turbines to the same theoretical incoming wave power, is around 10%. Some researchers are still working on improving the efficiency [18].

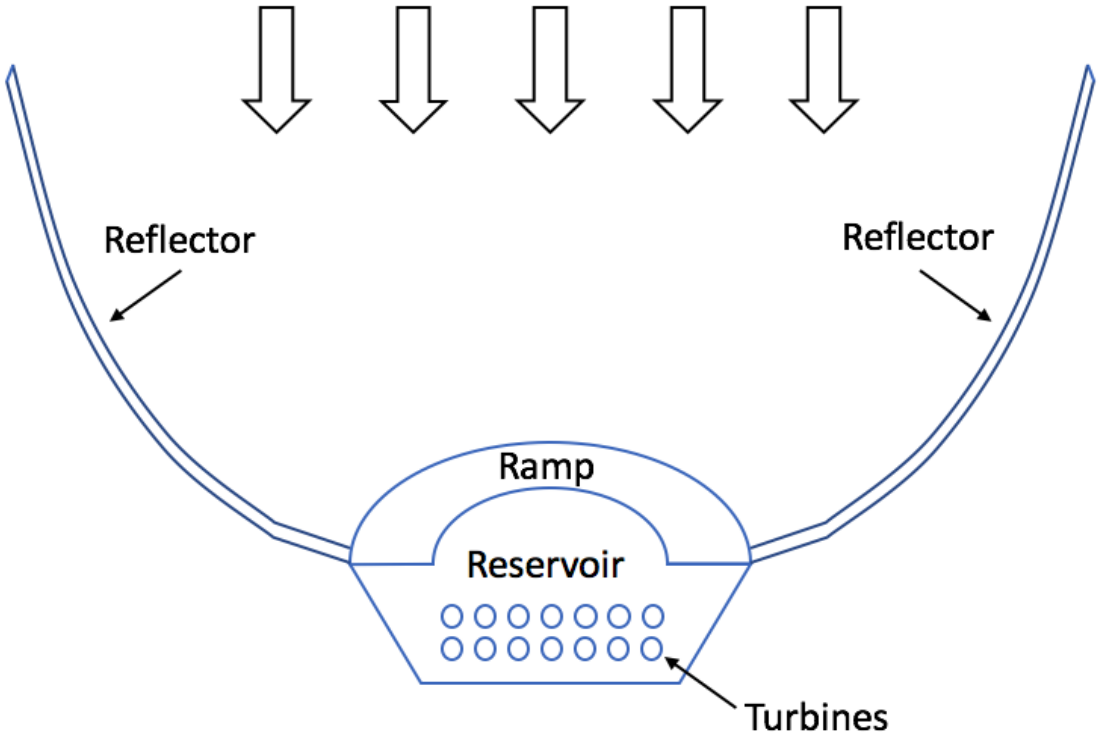

Figure 2. Original Wave Dragon with Reflectors reprinted from [19]

1.4 Smart Material

The objective of the thesis is to find an innovative way to improve the OWECs. Therefore, a type of smart materials is going to apply on an OWEC. Smart materials which are also called “Shape Memory Materials” (SMMs). They have the ability to memorize

their previous form after they are changed with an alter from the outer environment such as stresses, temperatures, moistures, pHs, electric, or magnetic fields. “Shape Memory Alloy (SMA)” which is one of the SMMs has been chosen. SMAs have been applied in several areas such as automotives, aerospaces, robotics, biomedicals, and others. The SMA is able to lift more than 100 times of its weight [20]. Briefly speaking, one can imagine a small diameter spring which is made by the SMA as human’s muscle and it can be transformed when alter comes in.

Recent research works have shown that the SMAs are better than conventional actuators such as motors, solenoids, pneumatics, and hydraulics [21], due to their unique characteristics and ability to react directly to environmental stimuli [22]. Flexinol, one of SMA manufacturers, indicated that SMAs are cheaper, smaller and easier to use when doing some small motors or solenoids [21]. But, there are still some challenges need to be overcome such as their limitations including a relatively small usable strain, low actuation frequency, low controllability, low accuracy and low energy efficiency [20]. In addition, although it is easy to achieve a rapid heating of the SMAs, there is no good way to cool down the whole system without drawbacks because of the limitations of the mechanisms of the heat conduction and convection. Due to the multiple transformation cycles, another big challenge is that the durability and reliability of SMA actuators. Some of the applications are significantly important to be insured for long-term stability, functionality, and safety such as in automotives [20, 23]. According to Flexinol, if the SMA actuators are used in appropriate designs, then obtaining repeatable motion for tens of millions of cycles is reasonable [21].

The spring which is made of the SMAs can be changed with its length by inducing a current is used in this work. The mechanism is that the spring is just like a resistant so that the temperature of the spring will be higher by powering on the current and cooler by powering off. As a result, the length will shorten or elongate to the desired length. Figure 3 shows the concept of the SMA. Figure 4 shows that one of the spring that made by the SMA.

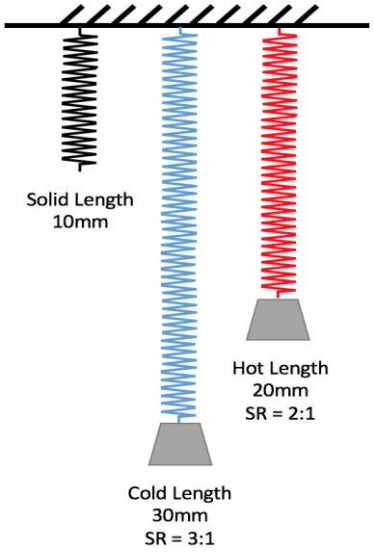

Figure 3. Example of Temperature-Control SMA reprinted from [21]

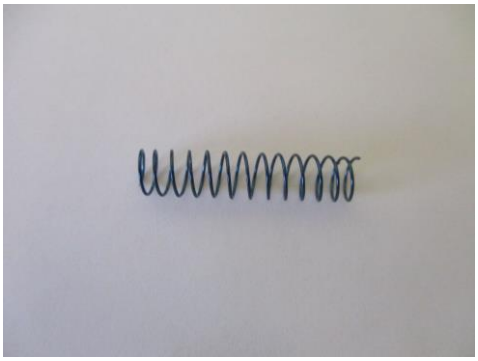

Figure 4. SMA Spring

In this thesis, a novel idea is that the ability to change the length of the SMA spring will be applied on an old type of OWECs. With the control of the temperature, the new OWEC can adapt to different wave conditions and improve the capability of gathering water. Thus, a physical model test will be conducted to confirm that the innovative material can improve the working performance of capturing wave power from the ocean.

1.5 Offshore Renewable Energy Station

1.5.1 Combine wind and wave energy converter

Because about 40% of the world population lives within 100 kilometers of the coast, it is reasonable to use the offshore wind and ocean energy as an alternative energy resource [24]. However, commercial wind or wave farms usually occupy large ocean space. It is more efficient to use the ocean space by combining the wind and wave energy converters together [25].

The advantage of the combined energy station includes the reduction of grid integration requirements, offshore transmission infrastructure capacity, and the cost of design and operation and the increase of the renewable energy yield of per ocean space [24]. However, there is no this kind of combined energy station operating in the ocean. There are still some challenges need to be overcome. First, the combination of two kinds of energy converters could increase the risk of accidents or damages such as a failure of mooring systems. Secondly, the lack of experience in co-located projects and the site-

selection. Thirdly, the early stage of the development of wave energy converter technologies will increase the cost [15].

1.5.2 Combine the OWEC with existed wind turbine platform

The objective is to make a wind turbine platform surrounded by OWECs so that the OWECs just like an extra part of the platform which can lower the cost without building another entire WEC system. The idea is that the wind turbine platform can act as the reservoir for the OWEC and both of them can use the same mooring system. At the same time, the reflectors can be uninstalled because the wave directions in the deep-water region don't change a lot during the year so that the waves from the main direction can be gathered. Figure 5 simply shows the new idea of the combined offshore renewable energy station. The upper part is the wind turbine and the lower part is the OWEC with smart material.

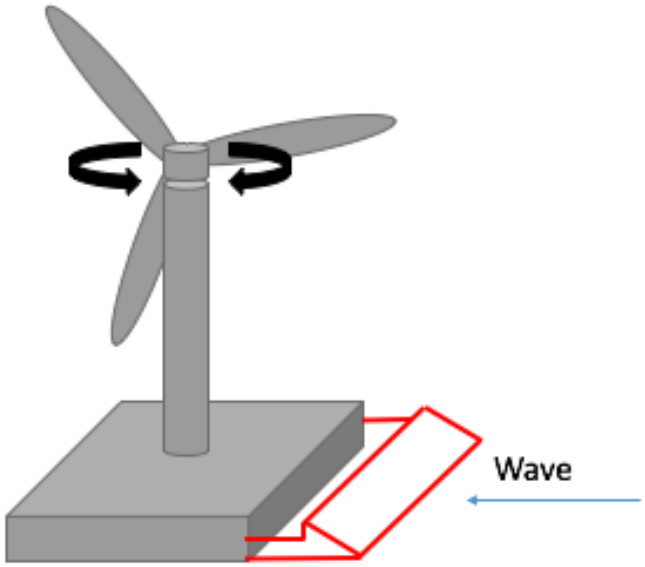

Figure 5. New Concept of Combined Renewable Energy Station

Another advantage of this new kind of energy station is that the wind turbine platform is pretty heavy so that the response when the wave across the structure and the design of the mooring system need not be concerned too much. The movement of the device will induce a different phase with the wave. This will possibly reduce the amount of the overtopping discharge. A laboratory test has indicated that the overtopping discharge will be reduced by up to 50% because of the movement of the floating structure [26]. At the same time, by reducing the oscillation of the device will prevent the water in the reservoir from spilling out. However, an extra WEC is just the simplest idea. Other kinds of renewable energy device can also be installed on this new kind of energy platform such as solar power, current power, and so on.

However, the most challenge thing is the early stage of wave energy converter technologies. This thesis will present a new idea to improve the work efficiency of the OWECs with using the SMA and the result of the physical model test is also presented.

2. LITERATURE REVIEW

2.1 Concepts of Overtopping Structure

During the past several decades, original overtopping structures were made to protect humans and their properties at coastal regions so that the goal is focused on minimizing the overtopping discharge which means that it was built to prevent the water from overtopping the dikes. Figure 6 shows that the overtopping structure at a coastal area as a dike.

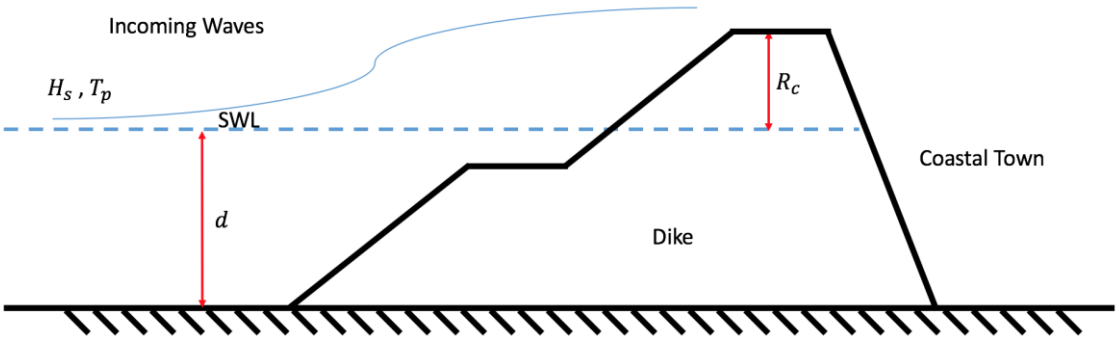

Figure 6. Overtopping Structure as a Dike at Coastal Region

2.1.1 General Formulae for Overtopping Structure

There are many experiments have been conducted with different kinds of setup. Most of them have come out with exponential equations to express the overtopping discharge. The one of them which is widely used is

$$Q = ae^{-bR}$$

where $Q\ (-)$ is the dimensionless overtopping discharge, $R\ (-)$ is the dimensionless crest freeboard height which is also called relative crest freeboard height, and coefficient a and b will be determined by conducting experiments.

According to Van der Meer and Janssen, a general formula can be expressed to descript the overtopping discharge with an impermeable, smooth, rough straight, and bermed slope [27, 28].

$$Q = \frac{q}{\sqrt{gH_s^3}} = 0.2e^{-2.60\frac{R_c 1}{H_s \gamma}}$$

where $q\ (m^3/s)$ is the mean overtopping discharge, $R_c\ (m)$ is the crest freeboard height, $H_s\ (m)$ is the significant wave height, and $\gamma\ (-)$ is the reduction coefficient which is introduced by the influence of berms, shallow foreshores, roughness, angles of wave attack, and etc. If there is no berm, no shallow foreshore, smooth slope, and head-on wave, γ should be 1.0. This equation is typically used when a breaker parameter is bigger than 2 because the overtopping discharge is reduced when the breaker parameter is smaller than 2 for the same wave situation.

2.1.2 Scale Effects on Overtopping

All the coefficients are determined by conducting experiments. For a scaled model test, scale effects should be concerned and investigated [29]. Because the wave overtopping phenomenon is dominated by the wave motion, a Froude modeling law governs. In the overtopping process, only a thin layer of fluid that viscous effect will

become important. This means that the influence of scale appears when small overtopping discharges occur.

2.2 Overtopping Wave Energy Converter

2.2.1 Concept of Overtopping Wave Energy Converter

Due to the different purposes of the coastal structure and the OWEC, there are still some differences between the two. The main purpose of the OWEC is to gain more water to harvest the power from the ocean.

In order to characterize the power that can be harvested from the OWEC, the structure can easily be described as the following picture. Figure 7 shows the concept of the OWEC and some of the parameters that will influence the overtopping discharge. The obvious difference from the defensive overtopping structure is that the OWEC doesn't extend to the seabed. This will affect the energy which can be got. The amount of water can be caught depends on several parameters such as significant wave height (H_s), peak period (T_p), crest freeboard height (R_c), ramp slope (α), draft (d_r), breaker parameter (ξ_o), and etc. The parameters which can be determined by the construction are R_c, α, and d_r. In 1991, researchers have already indicated that the R_c is more important than the α when lower and larger overtopping discharges occur [30].

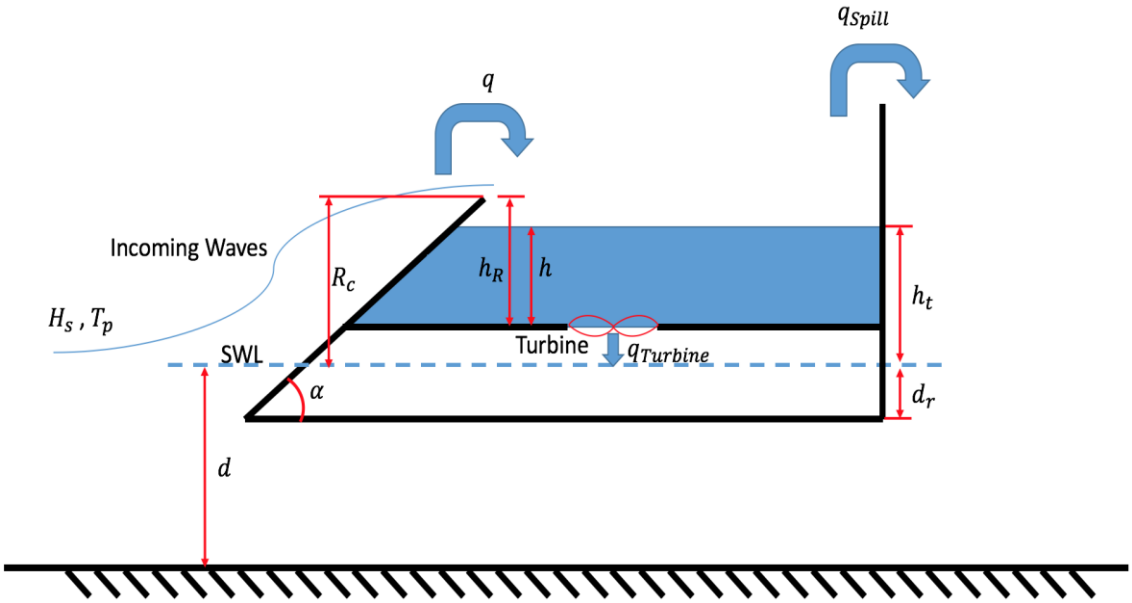

Figure 7. Concept of Overtopping Wave Energy Converter reprinted from [31]

In order to estimate how much power can be captured and to design the wanted structure, there are four steps that can be used to predict the final energy can be harvested [31]. First, the time-averaged potential energy of the overtopping waves (P_{crest}) is

$$P_{crest} = \rho \cdot g \cdot q \cdot R_c$$

where ρ (kg/m^3) is the water density and g (m/s^2) is the gravity acceleration. This formula means that the power of the wave needs to overcome the crest freeboard height to stay in the reservoir. Secondly, after the water is stored, the time-averaged potential energy which is the hydraulic power (P_{hyd}) and passes through the turbines at the bottom of the reservoir can be expressed as

$$P_{hyd} = \rho \cdot g \cdot q_{Turbine} \cdot h_t$$

where $q_{Turbine}$ (m^3/s) is the actual water pass through the turbines and h_t (m) defined as the difference between the water level in the reservoir and the mean water level (MWL). In addition, the h_t is necessarily lower than the R_c otherwise the water will drain back to the sea which means that the R_c also affects the capability of storing the water. Thirdly, the power produced by the turbines working at their optimal speed (P_{est}) is

$$P_{est} = P_{hyd} \cdot \eta_{turb}$$

where η_{turb} $(-)$ is the turbines' efficiency. The turbines' optimal speed can be derived from their characteristic curve by knowing h_t. Finally, the actual power (P_{act}), the power delivered to the grid, can be expressed as

$$P_{act} = P_{est} \cdot \eta_{PMG} \cdot \eta_{fc}$$

where η_{PMG} $(-)$ is the efficiency of the generators and η_{fc} $(-)$ is the efficiency of the frequency converters.

Among all the formulas, both of the first and the second equations dominate the power which can be harvested from the ocean wave. For the first equation, once the power of the wave crest is known, the relation between the q and the R_c can be obtained. The larger the q, the faster the reservoir can be filled. The second equation is related to the ability that the device can keep the water in the reservoir. The more water can be stored, the bigger value of the h_t can be got which means the higher P_{hyd} it can be. The third and last equations are about the actual electricity generation which depends on several efficiencies and is not the main concern of this research.

2.2.2 Maximize the Overtopping Rate of Overtopping Wave Energy Converter

As the result from the first two equations of the previous section, if the water level in the reservoir is much lower than the crest freeboard, the energy is lost as the overtopping water has a lower potential energy. However, if the water level in the reservoir almost reaches the crest freeboard, the water volume from a large wave is unable to be kept and will flow back to the ocean, a loss of energy. Figure 7 shows the condition of the water spill out and the inflows and outflows for the OWEC [19]. Therefore, the total discharge that can be transformed to energy can be expressed as

$$q_{Turbine} = q - q_{Spill}$$

where q_{Spill} is the spilling discharge. The hydraulic power mentioned before is

$$P_{hyd} = g \cdot \rho \cdot q_{Turbine} \cdot h_t$$

and the h_t can be rewritten as

$$h_t = R_c + h - h_R$$

where h_R (m) represents the distance between the crest freeboard and the bottom of the reservoir and h (m) represents the distance between the water level in the reservoir and the sea water level (SWL). The hydraulic efficiency, the ratio of the hydraulic power and the incoming wave power, can be expressed as

$$\eta_{hyd} = \frac{P_{hyd}}{P_{crest}} = \frac{q_{Turbine}(R_c + h - h_R)}{qR_c} = 1 - \frac{h_R - h}{R_c} - \frac{q_{Spill}(R_c + h - h_R)}{qR_c}$$

where q_{Spill} (m^3/s) is the spilling discharge from the reservoir and flow back to the ocean.

To maximize this hydraulic efficiency, it is desired to fulfill the following things. First is to ensure that the reservoir is close to be filled up which means that to minimize

the second term at the right-hand side (i.e., $h_R - h = 0$) because the energy will lose if the water head in the reservoir is not high enough. Second is to prevent too much volume from spilling out from the reservoir (i.e. $q_{Spill} \cong 0$,).

In addition, from these equations, the amount of the overtopping discharge highly depends on the R_c. If the R_c is large which also means a larger capacity of the reservoir, more water can be stored but it will make waves harder to overtop. In contrast, if the R_c is small which also means a smaller capacity of the reservoir, it will make waves easier to overtop but less water can be stored. Thus, the perfect condition is that the R_c is adjustable to fit different wave conditions. Figure 8 shows the result of different wave conditions with different R_c.

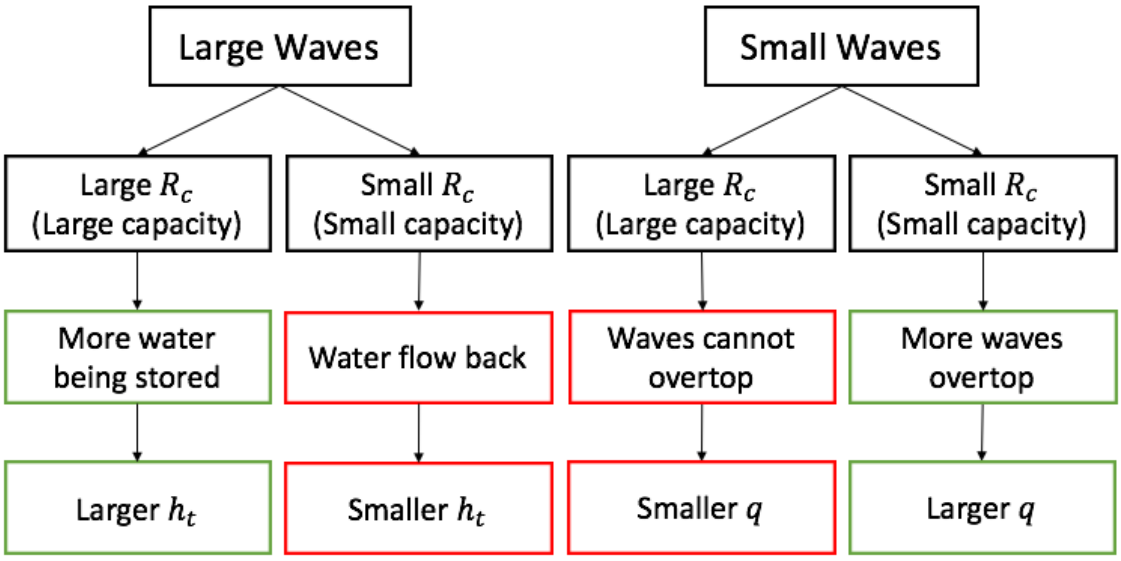

Figure 8. Different Wave Conditions with Different R_c

The best conditions are to have either large R_c for large waves or small R_c for small waves.

2.3 Effect on Overtopping Discharge

From the previous sections, the R_c is one of the most important parameters which dominates the overtopping discharge rate. However, there are many other parameters affect the discharge as well. All of them can be divided into two categories which are determined by the environment and the construction.

2.3.1 Effect of the Wave Climate

One of the environment effects is the wave condition. For an oblique wave, the influence of the angle of the wave attack is getting more important when the crest freeboard is higher. Most of the cases will get the maximum overtopping discharge when the head–on waves occurs which means an increase in the angle of the wave attack will decrease the overtopping rate [32].

The multidirectional waves give smaller overtopping rate than unidirectional waves for the normal incident condition [33].

Also, different spectral shapes will provide different wave conditions. Generally, the model tests for overtopping investigations use standard wave spectra such as JONSWAP which apply to offshore conditions or conditions with simple foreshores [34, 35]. From Schuttrumpf, he concluded that the multi-peak wave spectra which is based on the influence of the complex morphology. Therefore, the peak period is useless for the description of the wave run-up and wave overtopping and more meaningful to use the mean period instead when discussed the multi-peak wave spectra [36].

2.3.2 Effect of the Wind

Another environment effect is the wind condition. Wind effects can be negligible when an extreme overtopping happens, but the wind plays an important role when the small overtopping discharge occurs. Wind effects are more evident on steeper slopes [37]. In addition, according to J. A. Gonzales, a strong wind cause wind effects and the overtopping rate at logarithmic scale is proportional to the square of the wind velocity [38]. From recent research, the overtopping rate with the wind effect is 1.2 – 6.3 times of the one without the wind effects for sloped structures [39].

2.3.3 Effect of the Roughness and Permeability

There are several constructive factors will affect the overtopping phenomenon. Obviously, the introduction of the roughness and permeability of the slope will decrease the overtopping rate. Several investigations have been presented. Different kinds of armor unit will provide different roughness and porosity which need to be tested to get further information. The reduction coefficient will be taken into account when describing the overtopping rate [27, 28, 40-42].

2.3.4 Effect of the Crest Width

Generally, an increasing crest width will reduce the overtopping discharge. In some studies, the effects of the crest width have been introduced to the equations of the overtopping rate [32, 43]. From a recent test, sloped crest widths were investigated and the result showed the steeper the crest, the more discharge rate will be reduced [44].

2.3.5 Effect of the Slope Angle

Even though the slope angle becomes less important when the crest freeboard heights are lower or larger overtopping discharges occur, this parameter still influences the overtopping discharge all the time [30].

A wave run-up phenomenon is important when discussing the wave overtopping. The wave run-up will become the wave overtopping if the wave run-up is big enough. The maximum run-up occurs when the slope angle equals to 30° [45]. Most of the slopes are linear, but there are some studies for curving slopes. A convex slope increases the run-up height [46]. When the slope angle is smaller than about 35°, the effect of the slope angle is rather small [47]. For a limited draft and floating structure, Kofoed and Nielsen found that there is no significant variation with four different angles (35°, 40°, 45°,50°). None of the geometries were superior to a linear slope [48].

2.4 General Formulae for the Overtopping Discharge of OWEC

In order to predict the overtopping rate at different wave conditions, a predicted formula should be placed and concerned. Due to the complex and the non-linear nature of the wave overtopping phenomenon, overtopping flow predictions are normally based on empirical methods, mainly derived from experimental tests of reduced physical scale models. There are many studies are related to overtopping structure but few of them are related to the OWECs.

However, there is an empirical predicted formula that can be widely applied to the OWEC at different wave conditions and different geometries of the structures [34]. The

relative crest freeboard is ranged from 0.15 to 2.0. The geometry of the structure which is the slope of the ramp is ranged from $cot\,\alpha = 0.58$ to $cot\,\alpha = 2.75$ (about 20° to 60°).

$$Q = \frac{q}{\sqrt{gH_s^3}} = \lambda_{dr}\lambda_\alpha\lambda_s 0.2e^{-2.60\frac{R_c 1}{H_s \gamma}}$$

where all the λ terms are the correction coefficients. λ_{dr} is the coefficient at a different draft.

$$\lambda_{dr} = 1 - \kappa\frac{sinh\left(2k_p d\left(1-\frac{d_r}{d}\right)\right) + 2k_p d\left(1-\frac{d_r}{d}\right)}{sinh(2k_p d) + 2k_p d}$$

where k_p is the wave number based on the wave length of the peak period, L_p, d_r is the draft of the structure, and κ is found to be 0.4 by best fit. This is the largest difference with the coastal protective structure because the OWECs don't extend to the seabed. The energy flux which can be captured from the water column will be affect by the draft. The larger the draft, the more energy flux can be caught from the water column.

λ_α is related to the slope angle of the device.

$$\lambda_\alpha = (cos(\alpha - \alpha_m))^\beta$$

where $\alpha_m = 30°$ is the optimal slope angle and β is a coefficient equals to 3.

λ_s is varying with crest freeboard.

$$\lambda_s = \begin{cases} 0.4\,sin\left(\frac{2\pi}{3}R\right) + 0.6 & for\ R < 0.75 \\ 1 & for\ R \geq 0.75 \end{cases}$$

From the above equations, overtopping discharge can be enlarged by setting the parameters in the equations. There are three ways to make the goal. For the first equation is to increase the draft so that the device can get more energy during the wave go through

the area under the structure. For the second equation is to match the optimal slope angle which is 30°. For the third equation is to increase the relative crest freeboard to 0.75. By determining these equations and parameters, a structure with different demands can be designed by using different methods.

2.5 Previous Experimental Result of Overtopping Discharge

From the previous sections, the physical scale model test still needs to be done to determine the coefficients such as a, b, and γ.

One of the review papers shows that they have already done the test to collect the database with a floating model and three kinds of arms which are no arms, moving arms, and rigid arms. The model was scaled down from a prototype which operated in the North Sea. The model was designed to scale 1:51.8 [49]. The device was combined with a main body, a doubled-curve ramp, and two reflectors. The data was collected under irregular 2D waves from JONSWAP spectra-wave with a peak enhancement factor equals to 3.3, corresponding to the North Sea condition. Figure 9 shows the exponential lines of the model test. It is easy to see that with the help of two reflectors, the overtopping discharge will have a positive effect. However, all the three equations follow the general formula in Section 2.1.1 with different a and b.

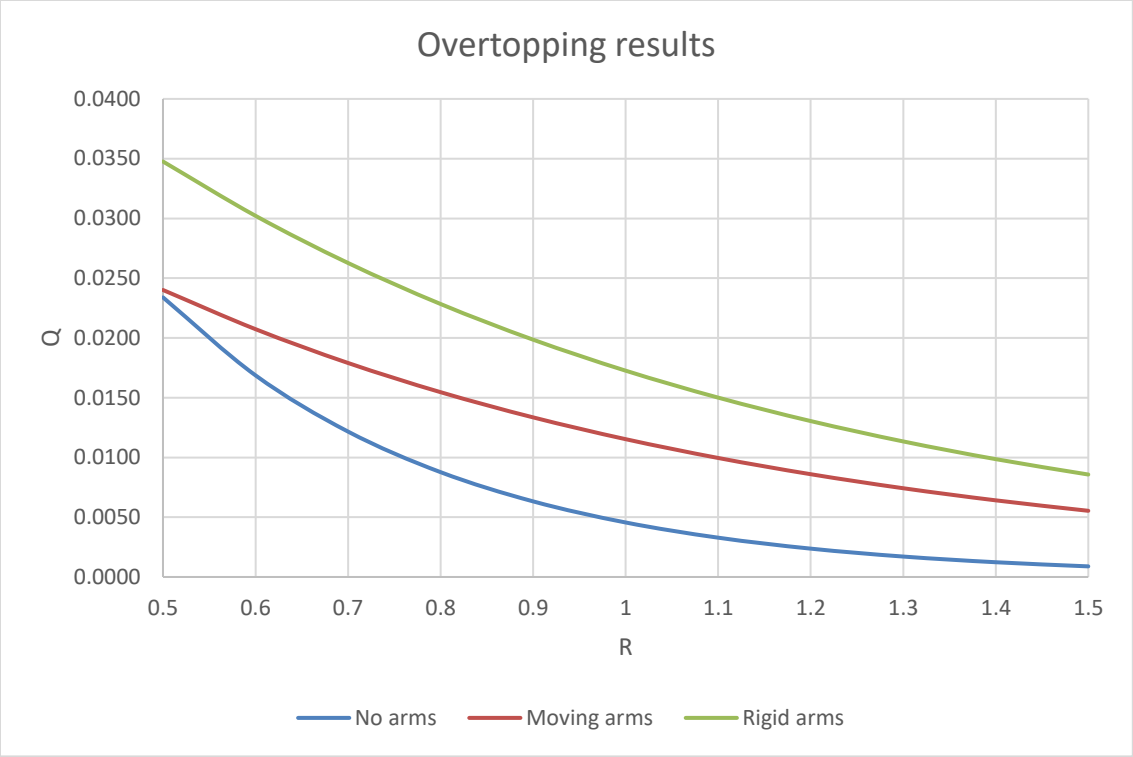

Figure 9. Overtopping Discharge from Borgarino reprinted from [49]

The equations are

$$Q_{No\ arms} = 0.12e^{-3.27R}$$

$$Q_{Moving\ arms} = 0.05e^{-1.467R}$$

$$Q_{Rigid\ arms} = 0.07e^{-1.40R}$$

The range for these equations is $0.5 < R < 1.5$.

From the visual observation, R between 0.6 and 0.9 is the best region for the water gathering. In this range, there is no important motion, no sinking, and no discharge spilling. There are different phenomena for different R. For a larger R, the waves are difficult to overtop the ramp and cause a less overtopping discharge. On the other hand, a

smaller R has a very large overtopping flow, the capacity of the reservoir and discharge pipes may be insufficient and the water will spill out.

3. NEW IDEA OF USING SMART MATERIAL ON THE OWEC

3.1 Apply SMA on the OWEC

In order to conquer the low efficiency of the OWECs, some innovative ideas should be applied to the systems. Because the OWECs have been chosen as the foundation of this thesis, some important parameters which are mentioned in Chapter 2 need to be more controllable to improve the efficiency.

Because the R_c is the most influential parameter which will affect the overtopping discharge rate, the most reasonable way is to adjust the R_c to fit different wave conditions. There are some methods that can change the R_c of the device. The easier and most common way is to change the slope angle by applying a hinge at the bottom of the slope and it will come with a changed R_c, but there is no good way to change crest freeboard height individually without changing the α which may also influence the discharge [50]. Another way is applied on the prototype in Nissum Bredning which is called Programmable Logic Controller (PLC). PLC controls the blowers and the valves under the device to regulate the buoyancy. The floating height of the platform can be changed by around 20 cm every hour. The regulation allows the ramp to rise in the storm so that the power capture can be improved [19]. However, the method also comes with a changed d_r which means that the energy can be caught from the water column will be affected. Also, in the wind turbine platform, the d_r doesn't change all the time due to the heavy weight of the structure. It is hard to apply the PLC system to the combined offshore

renewable energy station so that there should be another way to change the R_c without changing the slope angle and the draft.

Therefore, the application of the SMA is to change the R_c solely. Changing the length of the ramp is one of the methods which can combine with the SMA spring by using its property of elongation and shorten. For instance, if there is a larger wave coming which means that the OWEC needs to have a higher R_c, all of the two old ways and the new way are compared as follow. The wanted R_c is 1.5m.

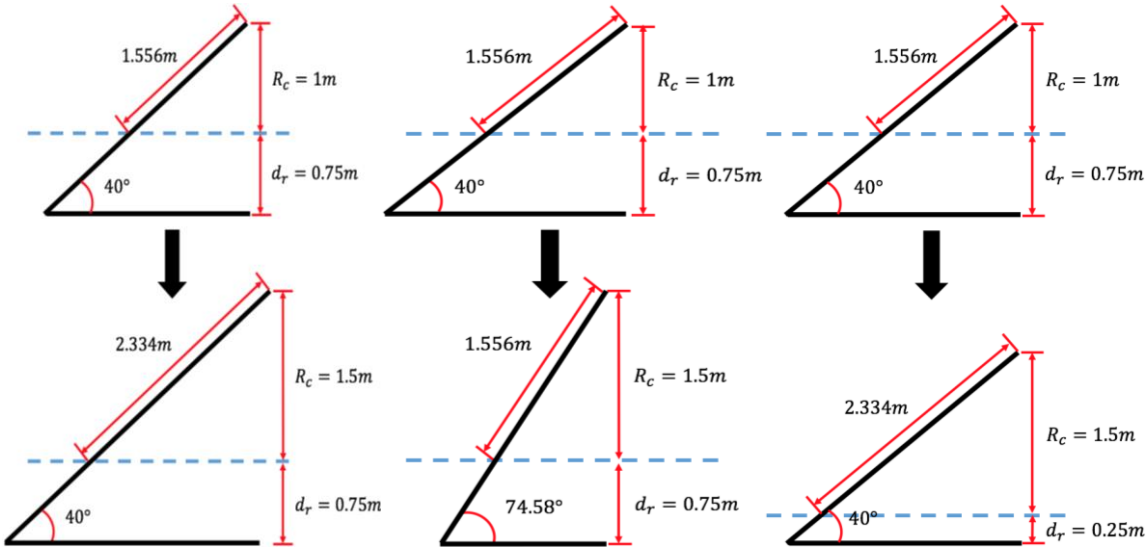

Figure 10. Change the Length of the Ramp (Left), Change the Angle (Middle), and Change the Buoyancy Height (Right)

In Figure 10, the right one shows that the changed R_c by changing the buoyancy height. The middle one shows the changed R_c by changing the angle of the slope and the left one shows the changed R_c by changing the ramp length. The advantage of changing the ramp length is that the angle is still fixed and the draft doesn't change. For the method of

changing the slope angle, the correction coefficient of the angle, λ_{α}, reduce from 0.955 to 0.361. For the method of changing the draft, the correction coefficient of the draft, λ_{dr}, reduce from 0.999 to 0.947. These will cause the overtopping discharge reduced by 37.8% and 94.8% respectively which will result in less overtopping discharge rates. Thus, the new method of changing the length of the ramp is more reasonable and efficient than the old methods.

The process is that during the operational time, the incoming wave data is collected and analyzed away from the device. After getting the analyzed wave data such as the H_s, the corresponding R_c will be determined to get the higher efficiency of the entire device. The length of the ramp can be adjusted by using the temperature-induced SMA. Therefore, the R_c is changed by deciding the temperature of the springs which is made of temperature-induced SMA to make them longer or shorter. At different temperatures, the springs can have different lengths so that the R_c can fit different wave conditions. For this thesis, the new kind of OWEC which is combing the old OWEC and the SMA will be tested.

4. EXPERIMENTAL SETUP

4.1 Experimental Device and Condition

4.1.1 Water Tank

The water tank for the physical model test is located at Civil Engineering Laboratory Building at Texas A&M University. The dimension of the tank is 0.9m wide and 36m long. The water depth can be filled up to 1.2m and the water tank is equipped with a flap type wave maker at one end and wave sponges at the other end.

A deep-water condition is assumed and the water depth is set to be 0.8m for the test. Based on the linear wave theory, kh need to be bigger than 3.2 which is dimensionless. Therefore, the period for the laboratory condition to fit the deep-water simulation is less than 1.01s.

4.1.2 Wave Maker

The wave maker is flap type and the wave period that can be generated is from 0.7 seconds to 4 seconds and the maximum amplitude is 1.2 volt. The calibration of the wave maker will be indicated in the following section. The device for sending an output signal to the wave maker and collecting input data of the wave elevation is an NI USB-6259 DAQ board. The programs for both output and input are programmed by the author.

4.1.3 Overtopping Wave Energy Converter

In order to conduct the physical model test, a scaled down model is built to fit into the water tank. Due to the limitation of the size of the tank, the reflectors of the OWEC are abandoned and make the device as big as possible to reduce the reflection from the

wall of the tank. The width of the device is built to be 0.85m and the length is 1.2m. Both sides have a gap with 0.025m. The draft for the case is 0.225m. Because of combing the OWEC with the heavy wind turbine platform, the structure is set to be fixed condition so that the motion of the device is not considered. Figure 11 shows that a rectangular base steel angle is put in the water tank to make the OWEC model fix on it. Figure 12 shows that the overtopping scaled down model which is made of acrylic sheets and sit on the steel angle.

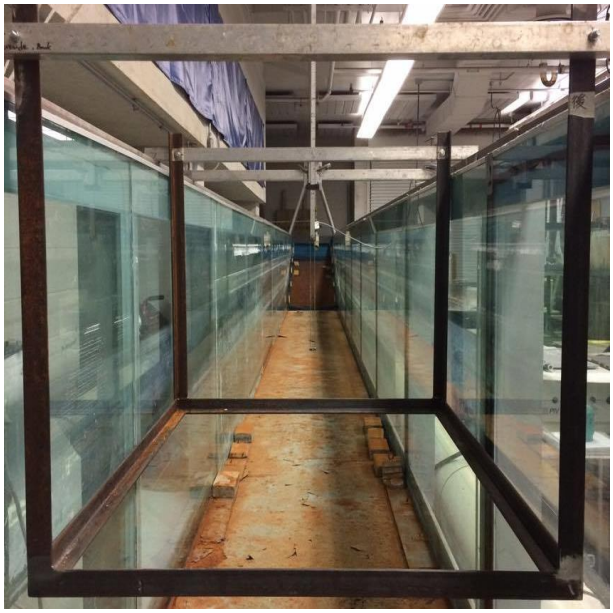

Figure 11. Steel Angle in the Water Tank

Figure 12. Scaled Overtopping Structure Model

The objective of the thesis is to confirm the feasibility of the SMA so other parameters need to be fixed except the temperature of the SMA. The angle of the ramp is fixed at 40° which has been widely used in other researches. They have already investigated that slopes between 35° and 60° and found that slopes between 35° and 50° do not have significant effects, but a slope of 60° only gives about 70% ~ 80% of the overtopping of a slope of 40° [34]. Figure 13 shows the sketch of the structure in the water tank and the location of the device.

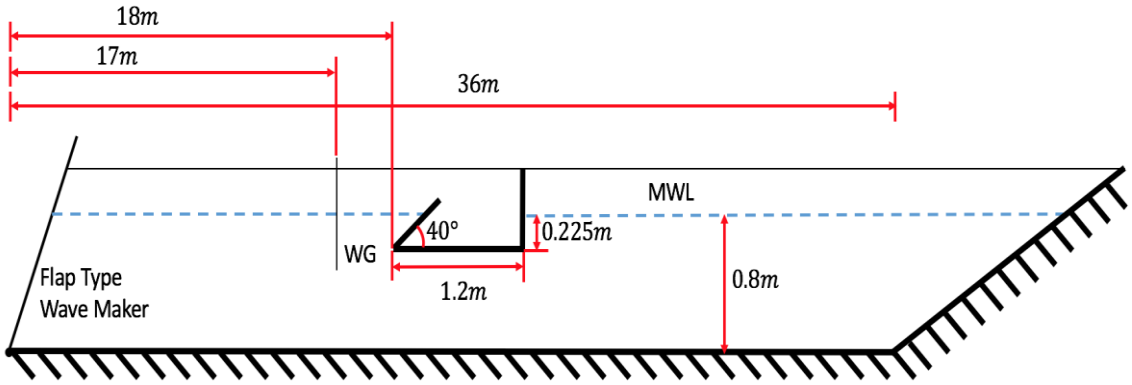

Figure 13. Sketch of the Water Tank and the Location of the Structure

After the water is harvested, there is a submersible pump at the reservoir of the device and the water will be pumped outside the wave flume into a box which is placed outside the water tank. By calculating the difference of the height in the box, the total discharge can be got. Then, the water will be pumped back to the water tank for the next experiment. Figure 14 and Figure 15 show the pumping system.

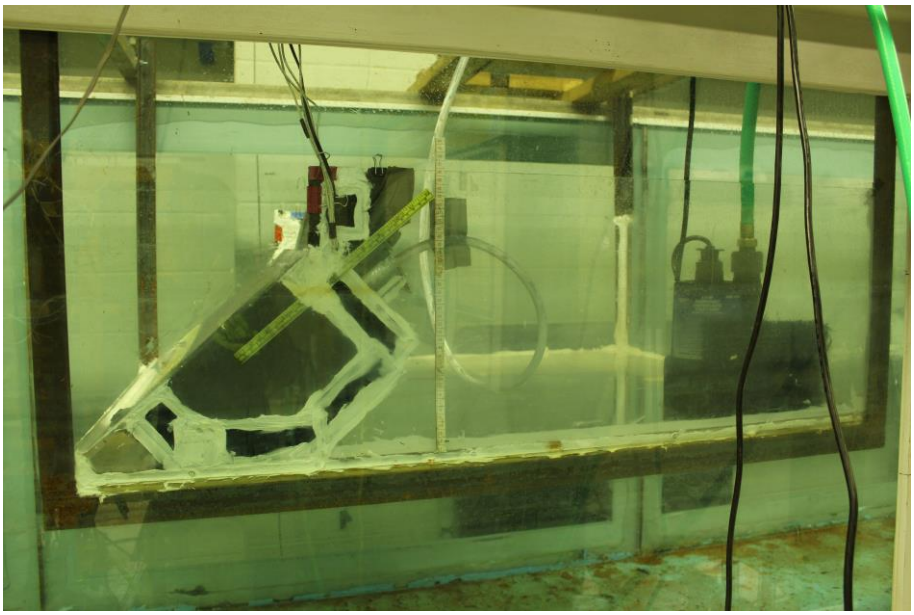

Figure 14. Submersible Pump in the Reservoir

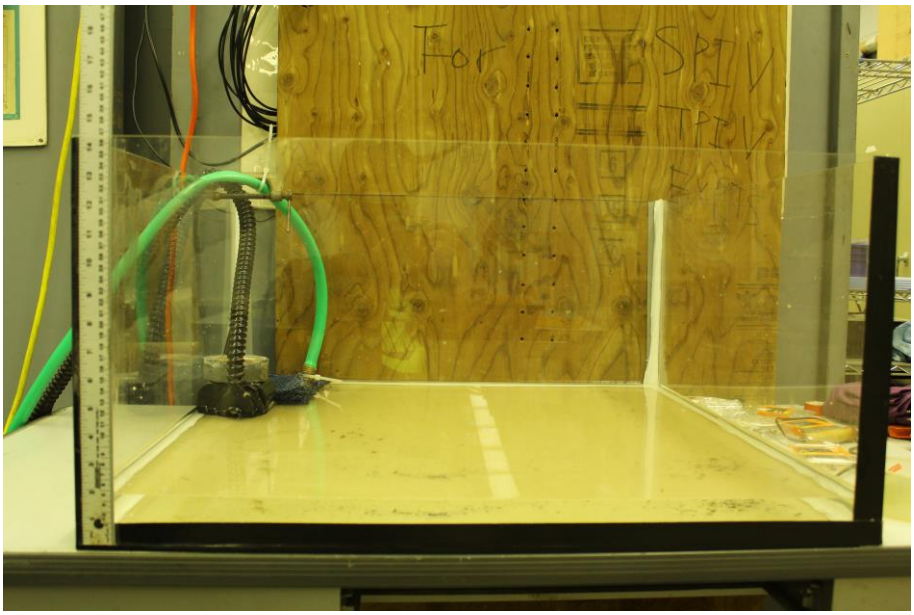

Figure 15. Submersible Pump Outside the Water Tank

4.1.4 Smart Material

The main purpose is to test the feasibility of the application of the SMA on the OWEC of changing the R_c by controlling the temperature of the SMA spring. In order to control and detect the temperature of the SMA spring, two power supplies, one contractor, and one temperature controller are used. Two sides of the springs are connected to two different rulers and one ruler is placed on the top of the fixed board, the other one is placed on the bottom of the movable board. The rulers are made of aluminum and the springs are welded to them. When heating up, the springs will shorten and bring the movable board up. When cooling down, the springs will elongate and bring the movable board down. Figure 16 shows the concept of the installation of the SMA spring.

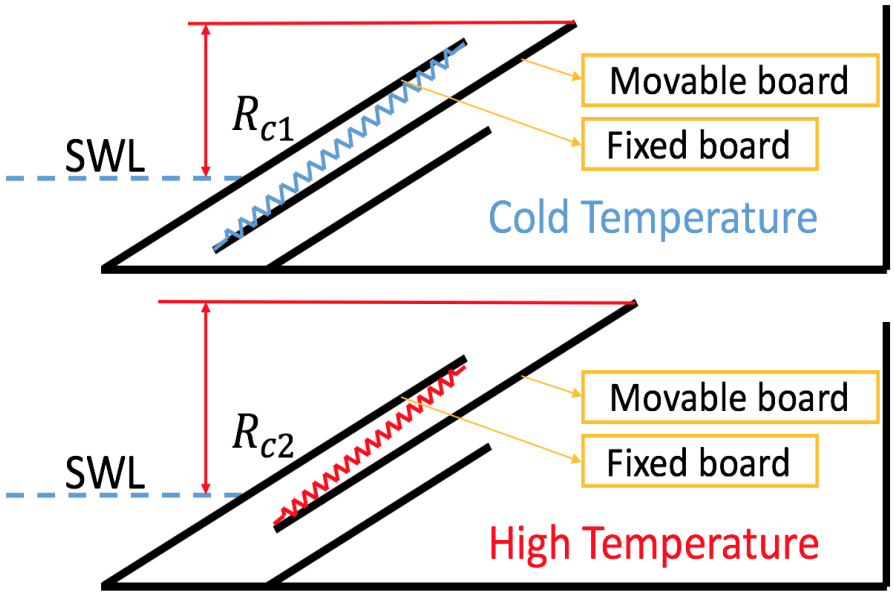

Figure 16. Concept of the Movable Board and the Fixed Board with SMA Springs

In order to make the electric current contribute to each spring more evenly, some copper foil tapes are used. The method is to control the springs at the desired temperature to get the wanted R_c. Figure 17 shows the power system which can control the SMA springs. Figure 18 shows the picture of the installation of the spring. Figure 19 shows that the temperature sensor is placed in the middle of one of the springs so that the sensor can detect the temperature more accurately. Figure 20 shows that there are rails between the boards so that the movable board can move with a lower friction force.

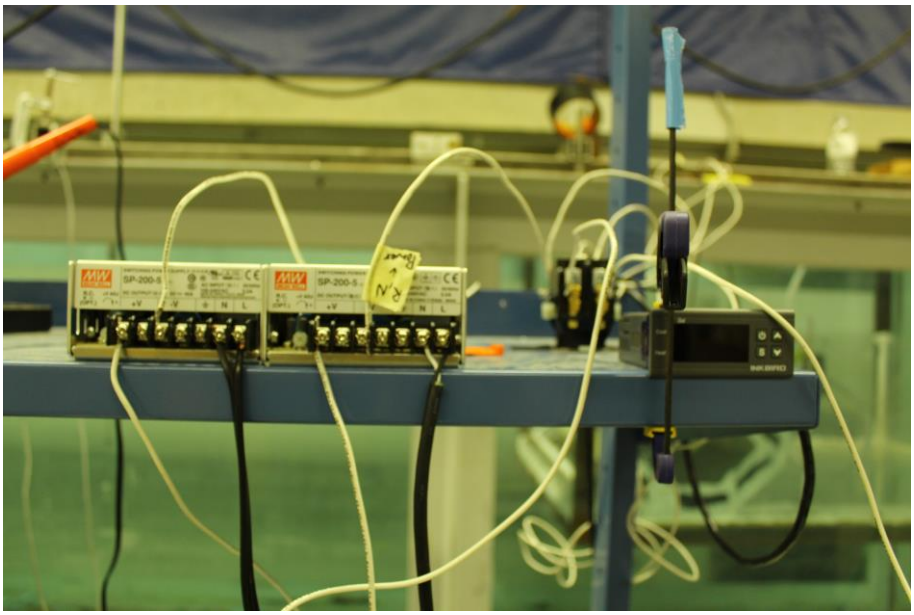

Figure 17. Power Supplies and Temperature Controller

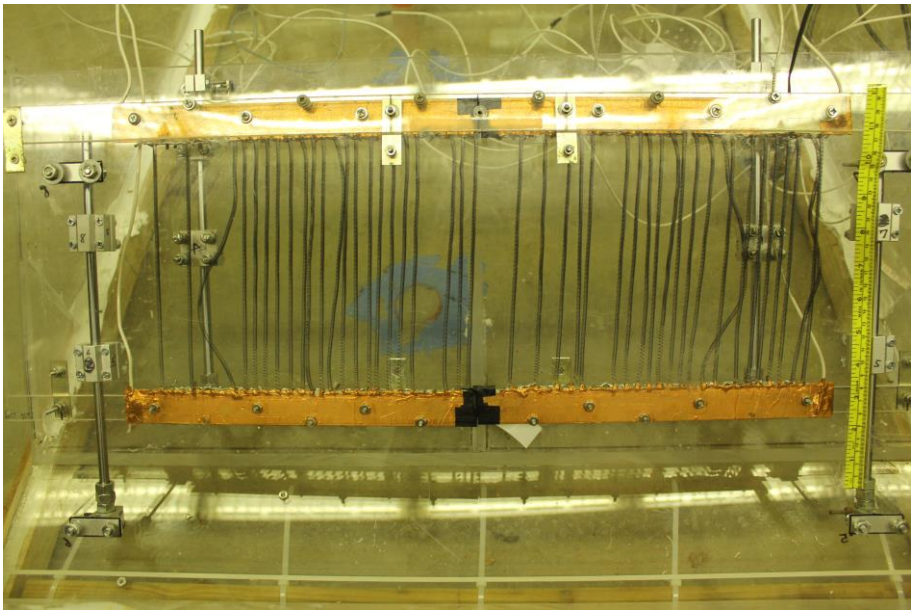

Figure 18. SMA Springs Installed on OWEC

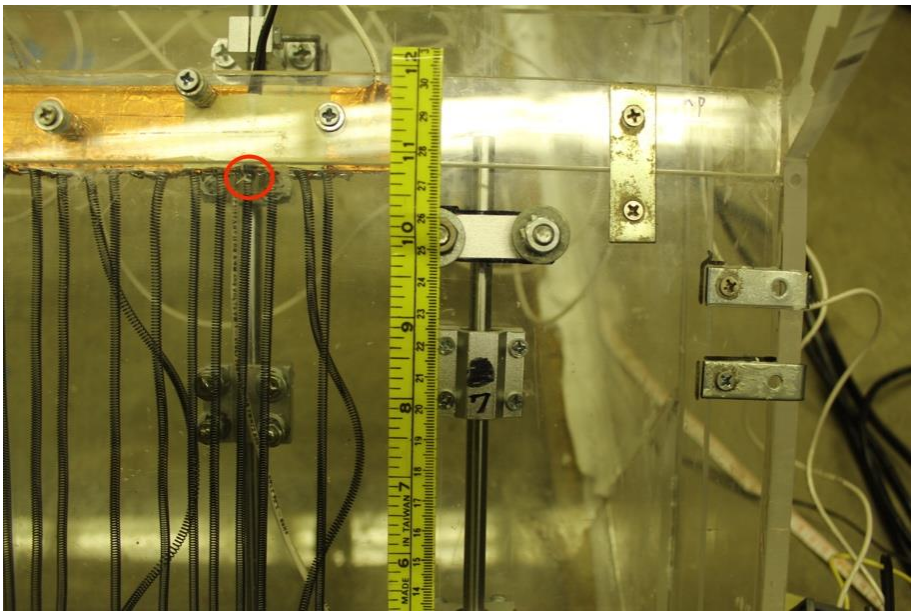

Figure 19. Temperature Sensor

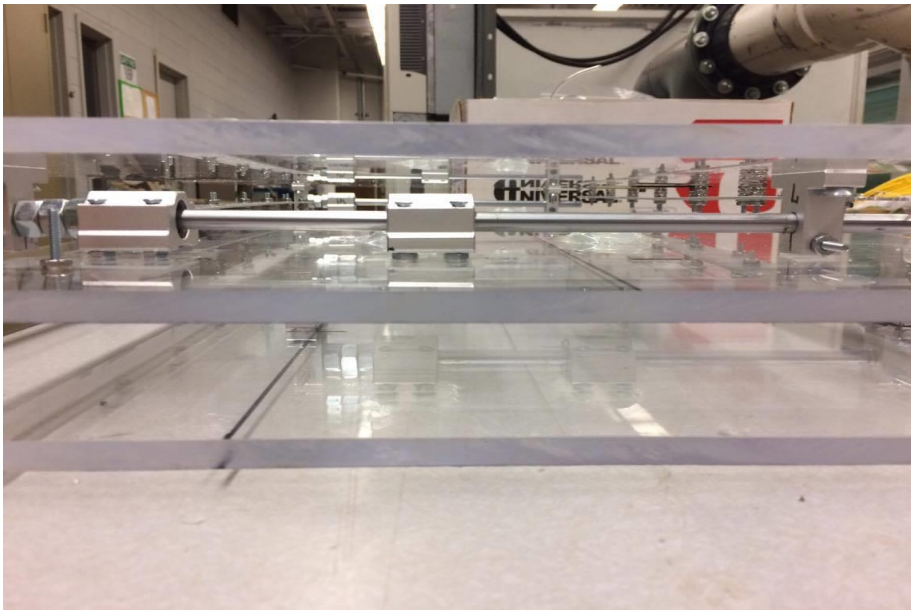

Figure 20. The Rails between Two Boards

After the springs are installed on the device, the sealing is going to be done to prevent the temperature from changing by the water. A small pumping system is applied to confirm that there is no water to disturb the springs. Figure 21 shows the device after sealing. Figure 22 shows the front view of the structure in the water tank.

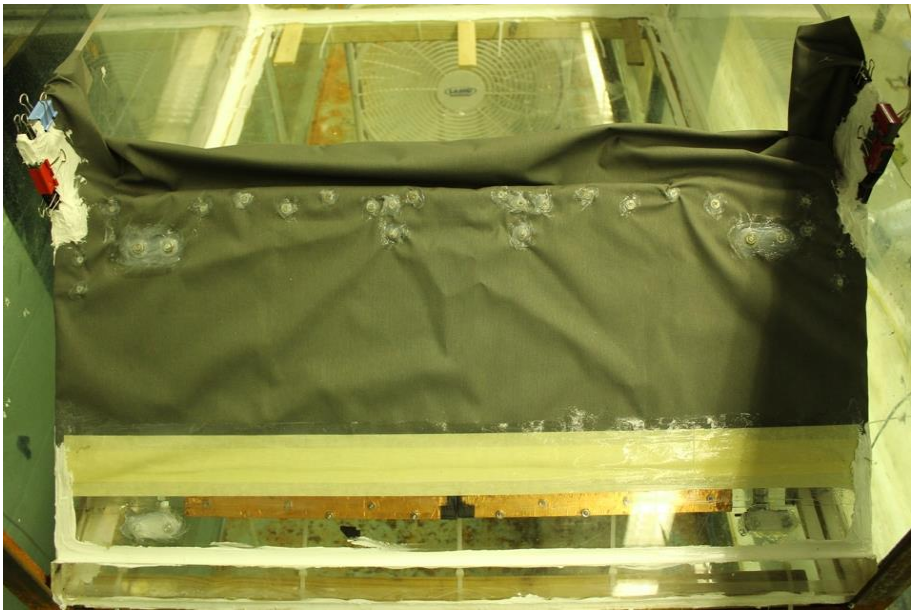

Figure 21. Sealed OWEC

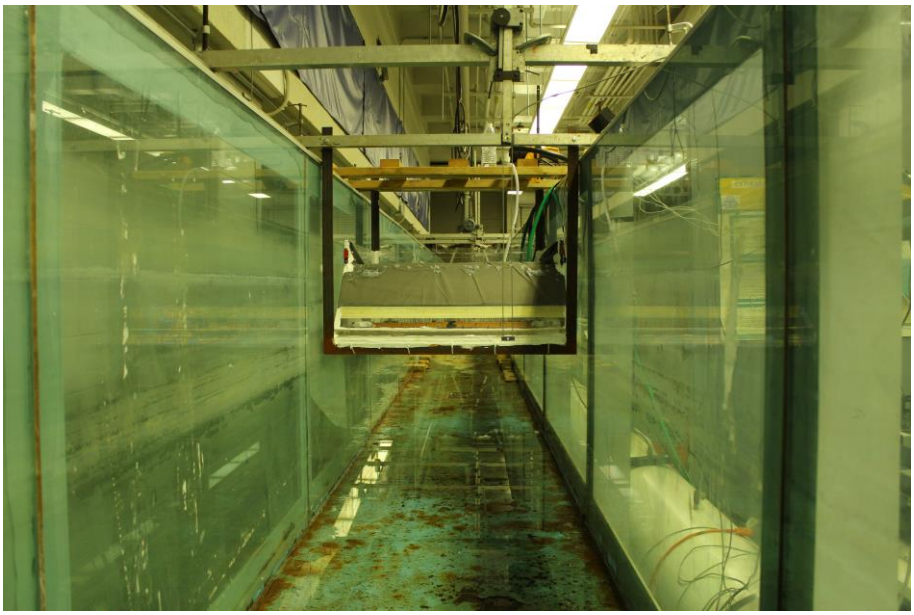

Figure 22. Front View of the OWEC

4.1.5 Experimental condition

For the wave conditions, the waves are irregular waves (i.e., JONSWAP spectra-wave). Thus, H_s is varied and based on the linear wave theory and the water depth in the water tank, the T_p equals to 1s to represent a deep-water condition. There are two kinds of conditions need to be done and compared. First one is to test with fixed R_c. The second one is the most important which is to test with switching on the smart material which means R_c can have different values. In the laboratory test, because of the limitation of the length of the flume, it is hard to place a wave gauge far away from the model to calculate the incoming wave property. Alternatively, one needs to send the wanted wave conditions to the wave maker and test the SMA springs function well at every condition, every R_c.

4.2 LabVIEW for Sending and Acquiring Data

All the tasks for sending output signals and acquiring input data are functioned by LabVIEW.

4.2.1 Output Signal to the Wave Maker

To trigger the wave maker, a new LabVIEW VI is programmed to send a time signal to the wave maker with an analog voltage output. In this VI, the regular wave (i.e. sinusoidal wave) is created by setting the duration time, the amplitude, and the period. There are two kinds of spectra-wave can be generated by setting the duration time, the significant wave height, and the peak period. In addition, a text file with digital signals can also be loaded to the VI. Figure 23 shows the VI is generating a JONSWAP spectra-wave.

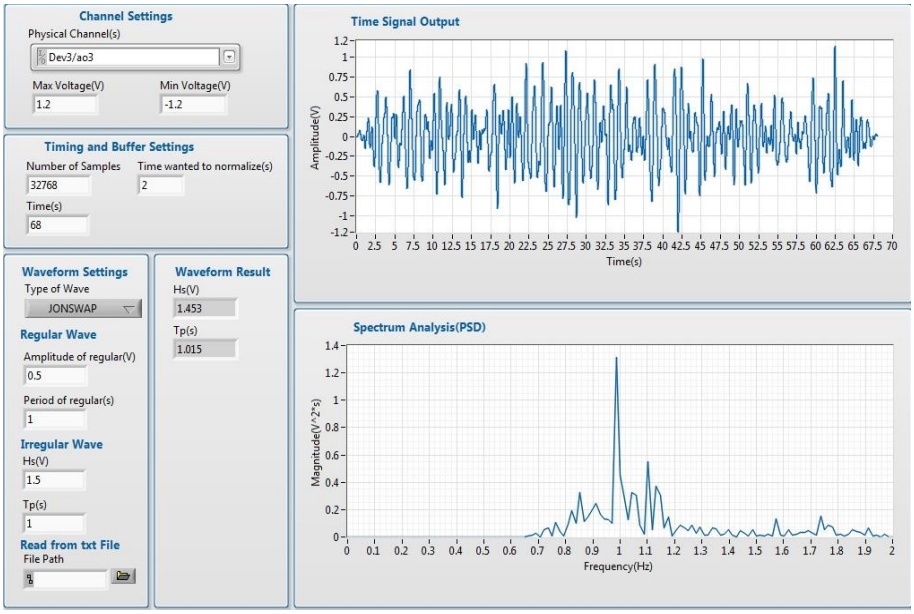

Figure 23. VI for Generating Output Signal

4.2.2 Data Acquisition and Spectrum Analysis

In order to know the parameters, H_s and T_p, in front of the device, the wave gauges are used to acquire the analog input of the time signal. The only parameter needed to be set is the duration time. In the VI, the program will receive the time signals and conduct a real-time spectrum analysis to get the H_s and the T_p. After getting the time signals, the data can be saved for future use. Figure 24 shows that the program is receiving the data from the wave gauge in the water tank.

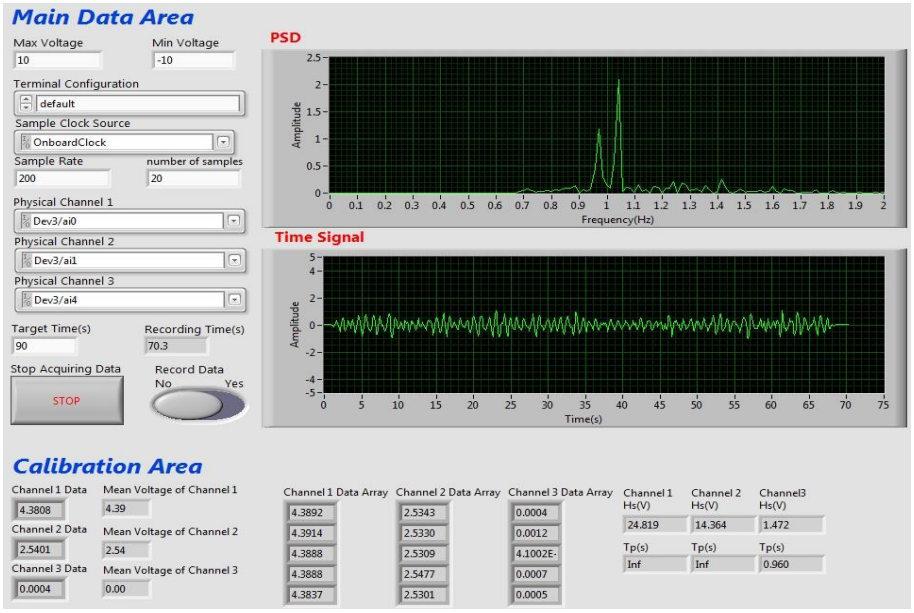

Figure 24. VI for Acquiring Input Signal

4.3 Wave Condition in the Laboratory

After the wave maker is calibrated, a table should be created which includes the wave heights in meters under different voltages and periods. In order to test the consistency of the wave maker, the regular waves are generated. Figure 25 shows that the

wave maker is more reliable for a period between 0.7 seconds to 2 seconds. Beyond this region, the wave maker will start to generate unreliable data and horrible noises which is due to the age of the machine.

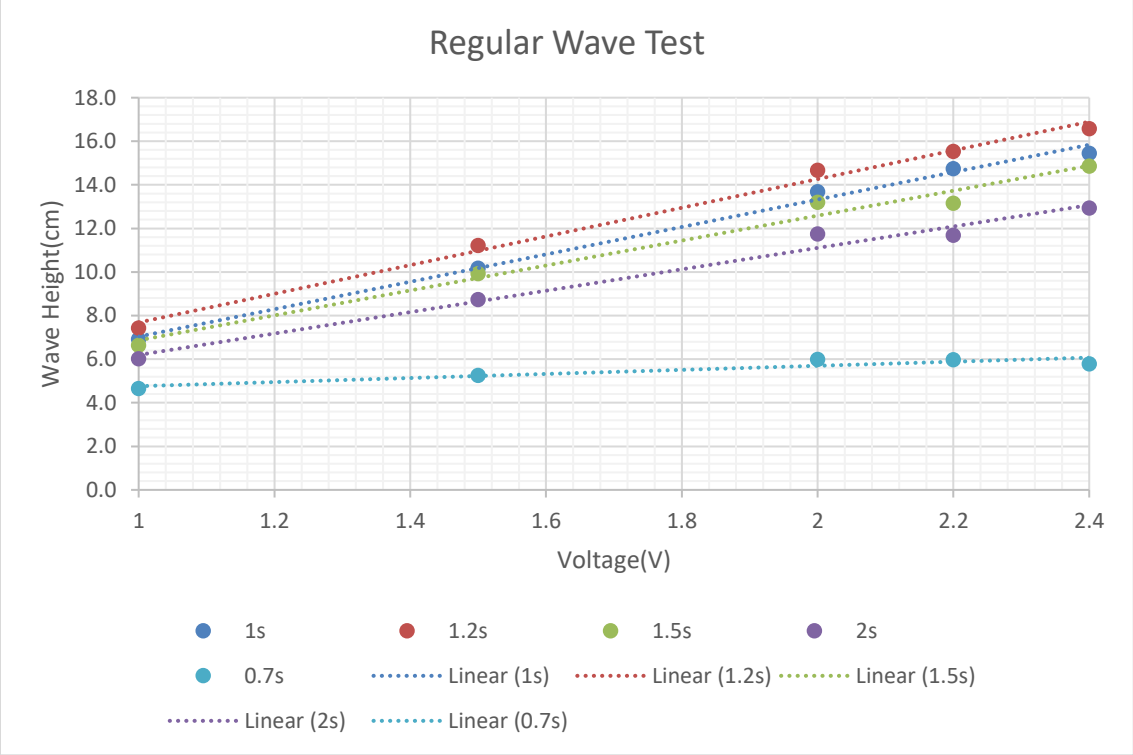

Figure 25. Regular Wave Test

For testing the stability of the wave maker under irregular waves, generating 600 seconds JONSWAPS spectra-waves with T_p equals to 1s at different voltages and find out the quasi-state times. As a result, in Figure 26, the signal will reach quasi-state after around 6 minutes.

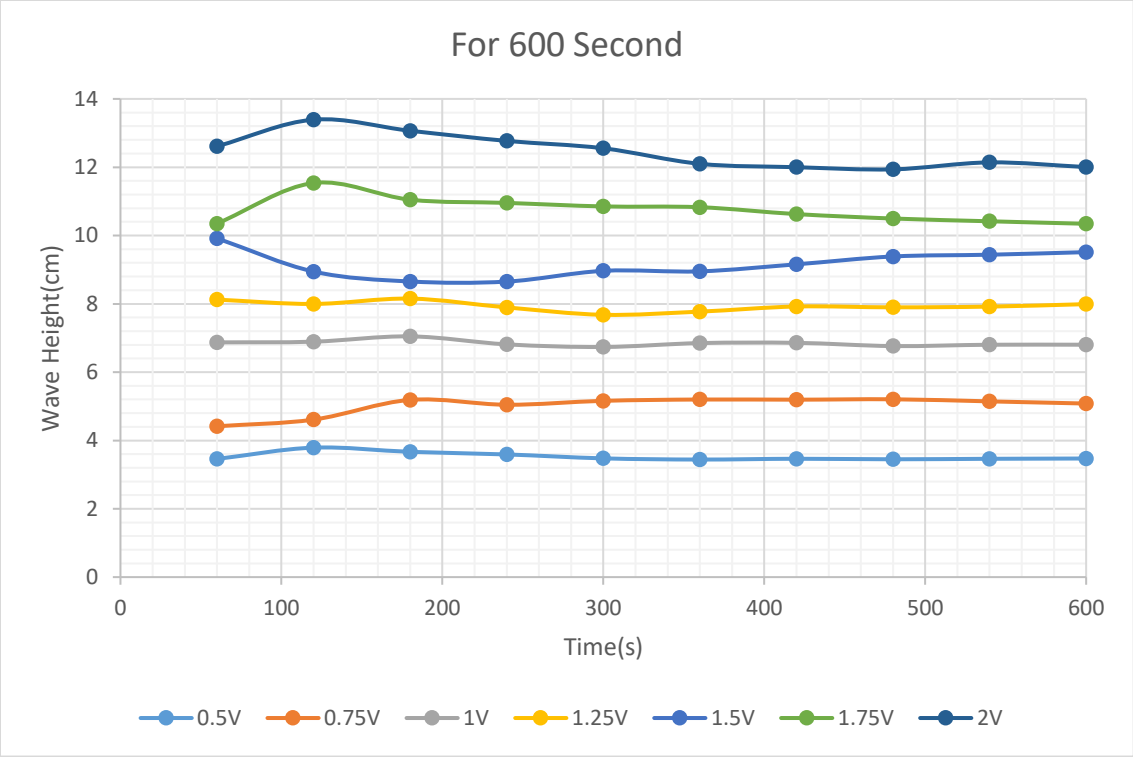

Figure 26. Wave Height for 600 second

Due to the restriction of the dimension of the water tank, it is hard to generate a wave with a longer time because of the complexity of the reflected phenomenon. The water tank equipped with the wave sponges at the end of one side of the tank. The distance between the wave gauge and the wave sponges is 19m. Although there are wave sponges to dissipate the wave power, the waves still reflect and cause the wave condition unpredictable. Alternatively, several shorter spectra-waves need to be created and combined to simulate a longer spectra-wave. Figure 27 shows that the wave elevation without the structure will be impacted by the reflected wave of the wave sponges after

around 30 seconds. The longer the duration time, the more complicated the wave condition it will be.

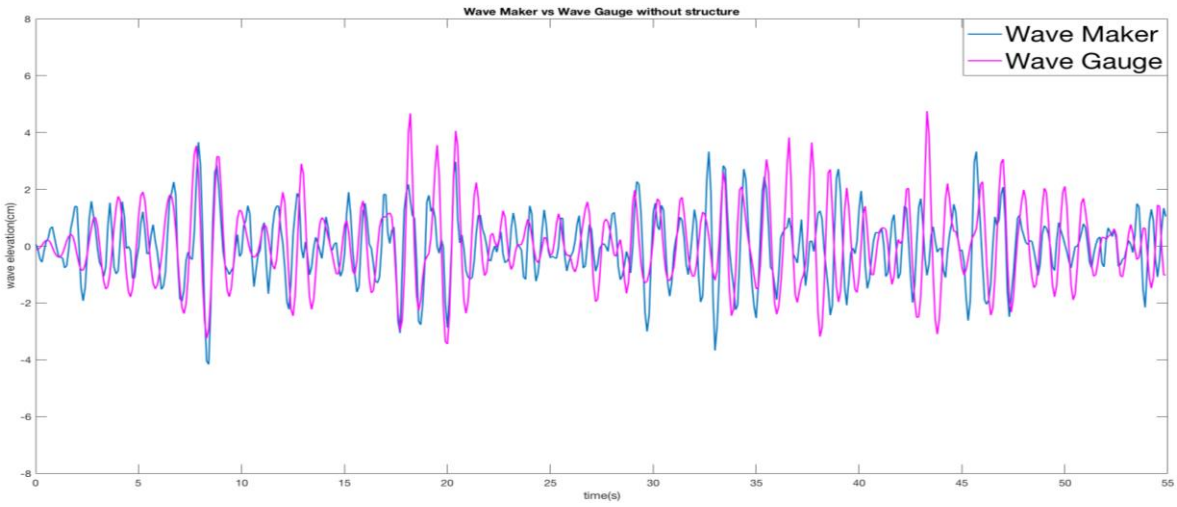

Figure 27. Wave Condition without the Structure

4.3.1 Real wave condition with structure in the water tank

Eventually, the output time for one dataset is determined by the location of the device which is 18m and the duration time is the time before the re-reflection wave hit the device and influence the data. Based on the group velocity, for 1-second peak period waves, the duration time until the re-reflection wave hit the structure is 68 second. After the structure is put in the water tank, the reflected phenomenon will be amplified because of the impenetrability of the device and the wave condition will be more unpredictable and complicated. In Figure 28, the wave condition with the structure is detected by the wave gauge and the figure shows that the wave elevation which is detected in the tank is much bigger than the signal which is calculated and sent to the wave maker. Therefore, it is not reasonable to use the detected wave elevation as the real wave condition. The

alternative way is to use the signal which is sent to the wave maker to calculate the real wave condition.

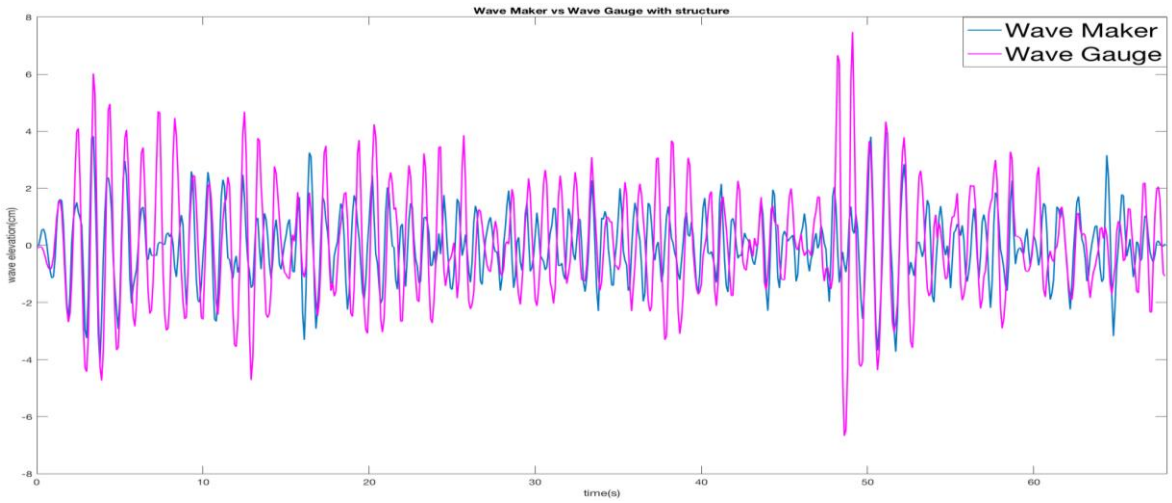

Figure 28. Wave Condition with the Structure

4.3.2 Error between output and theoretical value

However, one 68-second spectra-wave is too short to represent a good spectrum analysis so several 68-second spectra-waves will be generated to represent a longer spectra-wave. In order to compare the real output voltage to the theoretical voltage for the spectra-wave, a MATLAB file is used to calculate the error for the 1-second wave. Several 68-second spectra-waves are generated and combined together. With a longer-time signal, two methods are used to get H_s, one is the zero up-crossing method and the other one is spectrum analysis method. Both of them are done for 30 times and take average and standard error. In Table 2, the average of error and standard error for three 68-second, 204-second, spectra-waves are both below 5% which is generally acceptable for the

physical model test. As a result, three 68-second spectra-waves are generated to represent a longer wave which will be closer to the theoretical H_s.

# of spectra-wave		1	2	3
Average of Error (%)	Zero up-crossing	-3.1	-4.2	-2.6
	Spectrum Analysis	0.1	-1.0	-0.6
Standard Error (%)	Zero up-crossing	8.4	6.8	4.1
	Spectrum Analysis	8.3	6.4	4.1

Table 2. Error between Theoretical and Real H_s

4.4 Calibration of the SMA Spring

To get the exact R_c at the wanted temperature, the calibration of the SMA springs need to be done. The R_c have been recorded at different temperatures. The test has been done for several times to ensure that the SMA works.

4.4.1 Reliability of the SMA Spring

The first kind of tests is to gradually increase and decrease the temperature and record the R_c. Figure 29 shows that the trend of the location is similar for both heating up conditions and cooling down conditions. Compared with the strain data provided by the manufacturer of the SMA which shows in Figure 30. It shows that the tendency is similar but with some offsets. The result has a lower operating temperature and a larger operating strain. These differences come from the extra loading of the boards and other equipment. The test indicated that the function of the SMA spring is reliable. However, there is still a

little bit difference between each test. The difference comes from the friction force on the rail.

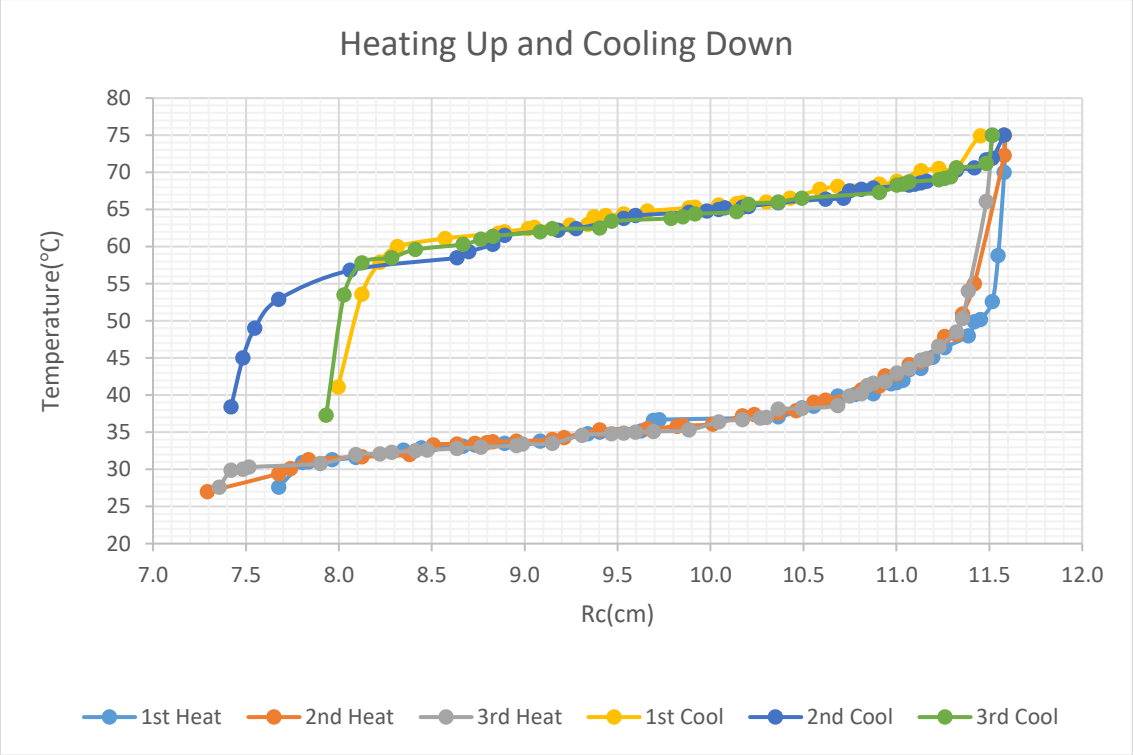

Figure 29. R_c for Gradually Heat Up and Cool Down

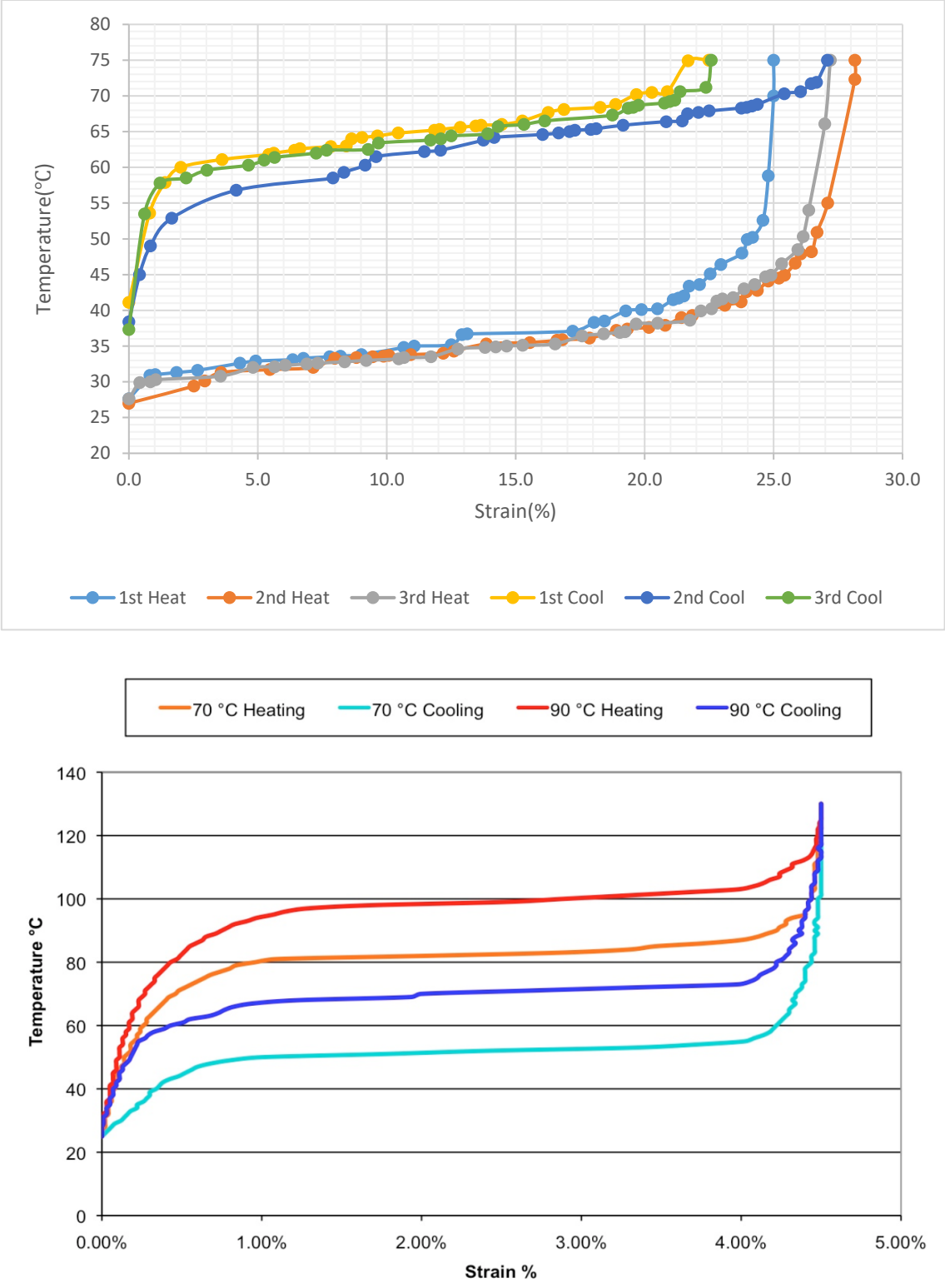

Figure 30. Compare the Strain with the Data from Manufacturer reprinted from [21]

4.4.2 Exact R_c at Different Temperature

The second kind of tests is to find out the exact R_c at different temperatures. This test is for that though the temperature of the springs has reached the wanted value, the air which surrounds the springs will make the springs' temperature fluctuate till the air temperature become stable and closed to the temperature of the springs. The test has been done in two different ways. The first three tests are set to be started from around 30℃ to the wanted temperature until it is a stable condition. The last three tests are set to be started from random temperature to the wanted temperature. Figure 31 shows that the first three tests are more reliable and consistent. The unreliability of the last three tests is caused by the different friction force at the different temperatures and different locations on the rails.

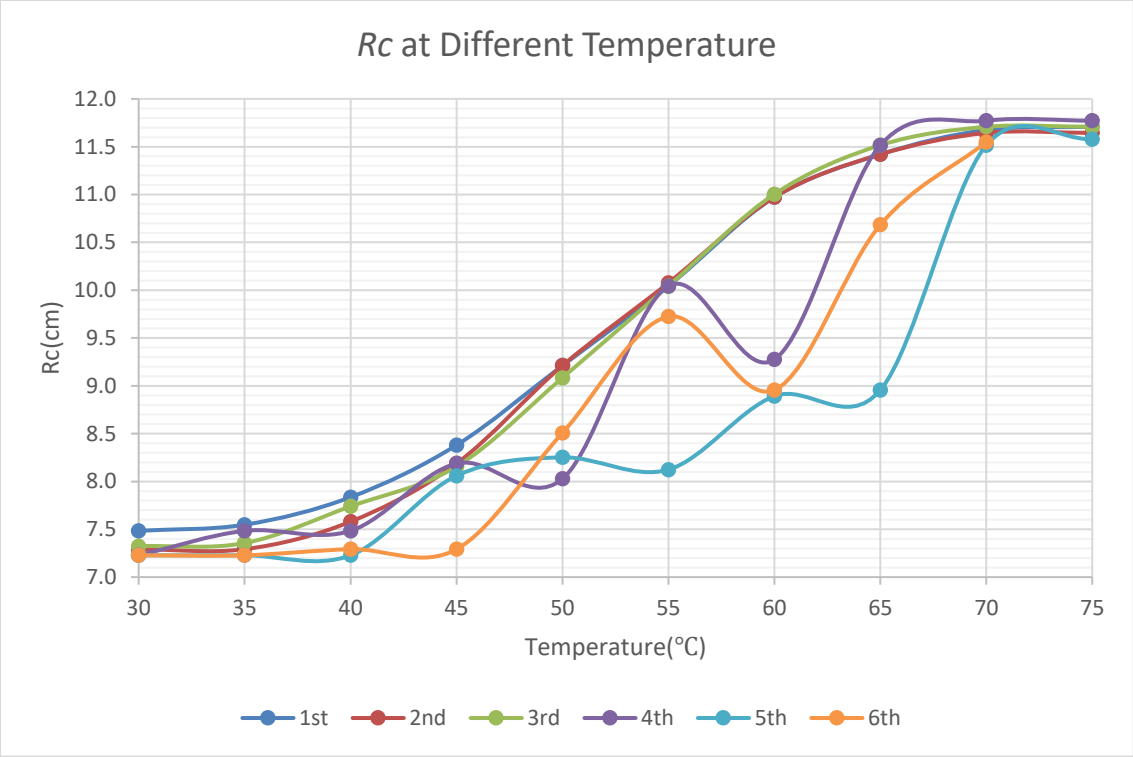

Figure 31. R_c at Different Temperatures

5. EXPERIMENTAL RESULT AND DISCUSSION

In order to compare the fixed and the adjustable R_c in the real physical model test, two kinds of experiments have been conducted. Because the water depth is 0.8m, from dispersion relationship for a deep-water condition, the wave period needs to lower than 1.01s. Thus, a peak period of 1 second has been selected. The wave pattern is JONSWAP spectra-waves. For each data point, the total overtopping discharge rate are gathered from three 68-second spectra-waves. The range of the experiments depends on R. The overtopping discharge rate is too small to accurately calculate when the R is bigger than 2.0. On the other hand, the overtopping discharge rate is too large to completely gather when the R is smaller than 0.5.

5.1 Fixed Crest Freeboard Height

For the fixed condition, which is the control group, R_c has been chosen to be 0.075m. The result of the fixed condition is compared with previous empirical formula (Borgarino 2007) and the general formula of the floating overtopping device (Kofoed 2002) [34, 49].

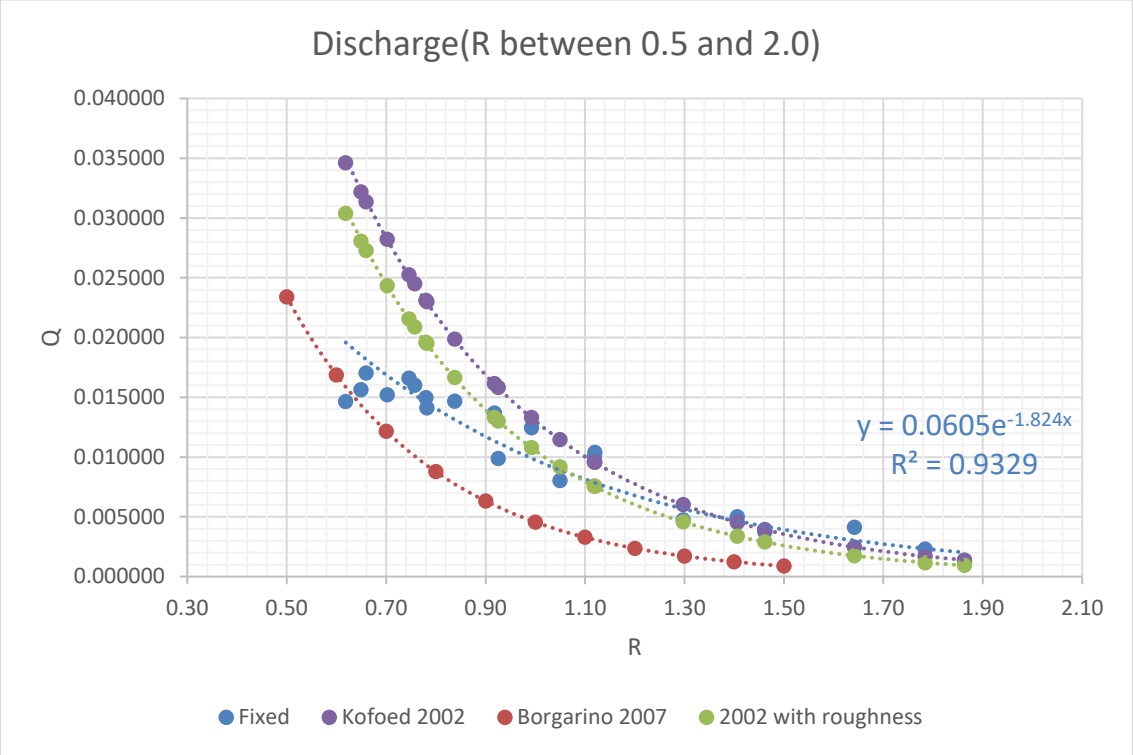

Figure 32. Overtopping Discharge at Fixed Condition

In Figure 32, the difference between the fixed condition result and the experiment result from Borgarino in 2007 is obvious. The dimensionless discharge of the new experiment result is much bigger at every value of the *R*. It is caused by the different setups of the experiment, but the tendency is similar. The most influential factor is that Borgarino's structure is floating so that the discharge rate will be affected by the movement of the device. In order to have more controllable parameters, the reduction coefficient and the correction coefficients, it is more reasonable to compare with the general formula of the overtopping device from Kofoed in 2002.

For the general expression from Kofoed in 2002, the correction coefficients are determined by the dimension of the device. Thus, the λ_{dr} is 0.919 and the λ_{α} is 0.955. In addition, the reduction factor for the general formulae is assumed to be 1 which means there is no penetration and roughness on the ramp. The purple line (general formula with γ equals to 1) and the blue line (the fixed condition) still have some differences. Reasons for the reducing and fluctuating discharge are following.

First, the phenomenon of the fluctuation of the same R is due to the run-down and run-up of the wave. The overtopping phenomenon is highly related to the wave run-up and run-down. For the wave which doesn't have enough run-up height to overtop the ramp, the run-down phenomenon occurs. After the wave reaches its maximum run-down point, a secondary run-up starts. This secondary run-up is much smaller than the first one, for the major portion of the wave has been reflected by the steep slope [51]. If the following wave has a same phase with the secondary run-up, it will increase the possibility of the upcoming wave overtops. In contrast, if the following wave has a different phase with the secondary run-up, it will decrease the possibility of the upcoming wave overtops. In addition, by observing, the water which doesn't overtop the ramp will flow back to the water tank and caused the water level set-down. The set-down will make the next incoming wave harder to overtop the ramp. The possibility of this phenomenon is determined by the randomness and the form of the random wave. Figure 33 and Figure 34 show the run-down and the run-up during the overtopping phenomenon.

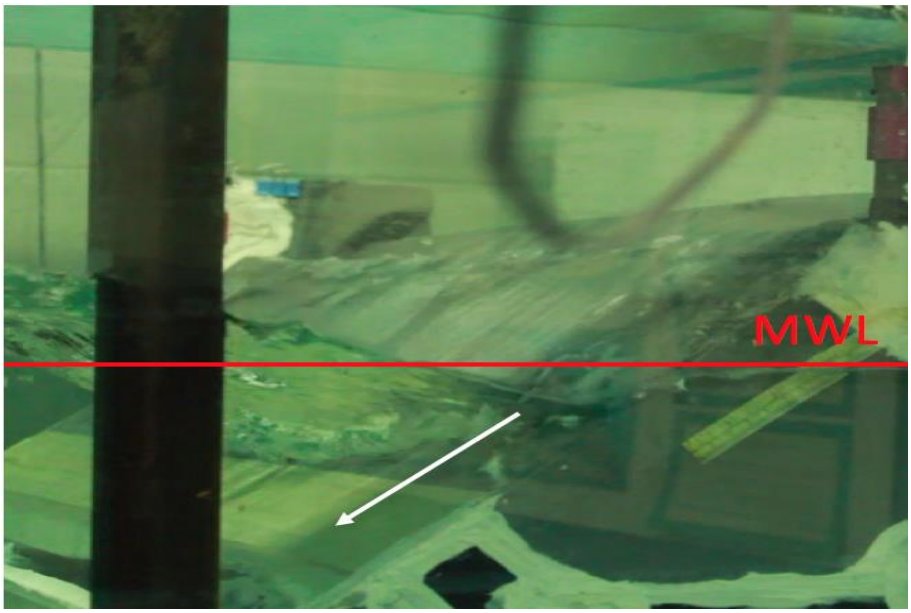

Figure 33. Run-down of the Wave

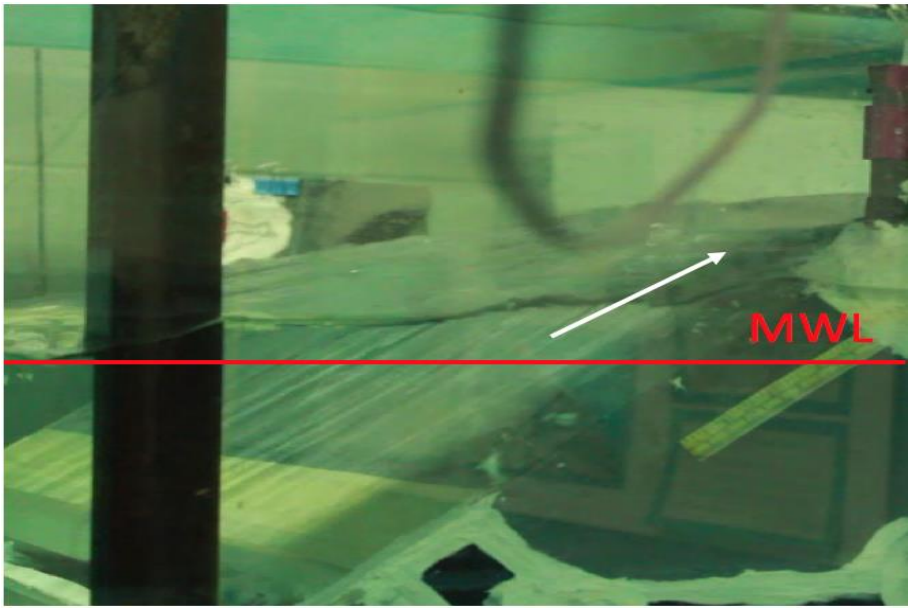

Figure 34. Run-up of the Wave

Second, because of the surface roughness of the ramp, vortices and bubbles will be created and dissipate the wave power. Figure 35 shows that when the wave rushed on the slope, the vortices and the bubbles will be generated.

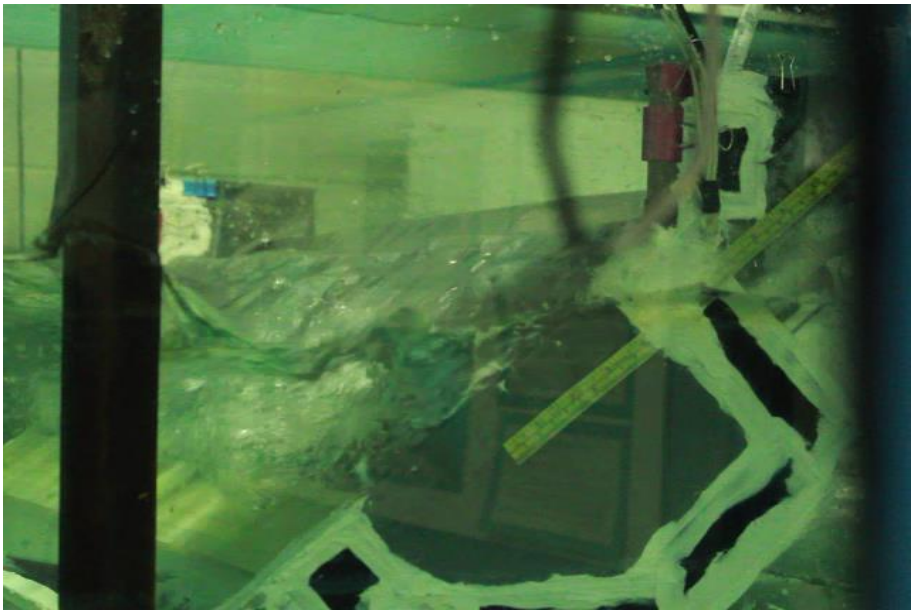

Figure 35. Vortex and Bubble at the Ramp

Therefore, it is more reasonable to take the roughness into account. For the green line in the Figure 32, the reduction coefficient is assumed to be 0.925. In order to compare which line is closer to the fixed condition, the averages of error are calculated from the R equals to 0.5 to the R equals to 1.5 because when a smaller R occurs, the scale effects should be concerned. The average of error for the purple line (no roughness) is -21.3% but for the green line (with roughness) the average reduces to -0.1%. This means that the green line is closer to the result of the fixed condition.

Third, another phenomenon is that when the R is big, the result is well fit but when the R is small, the difference is obvious. Because of the constraint of the experimental devices and the property of the random wave, waves are easier to break for bigger amplitude at a relative lower period. The energy will be dissipated after the wave breaks which means that the wave height will decrease and cause the wave hard to overtop the ramp. The bigger the H_s, the higher the possibility of the breaking waves occur. That is the reason why there is a bigger reducing discharge when a smaller R occurs. Figure 36 shows that the wave breaks just before the structure. Figure 37 shows that the wave breaks near the wave maker. Both of the conditions will lead to a reducing discharge.

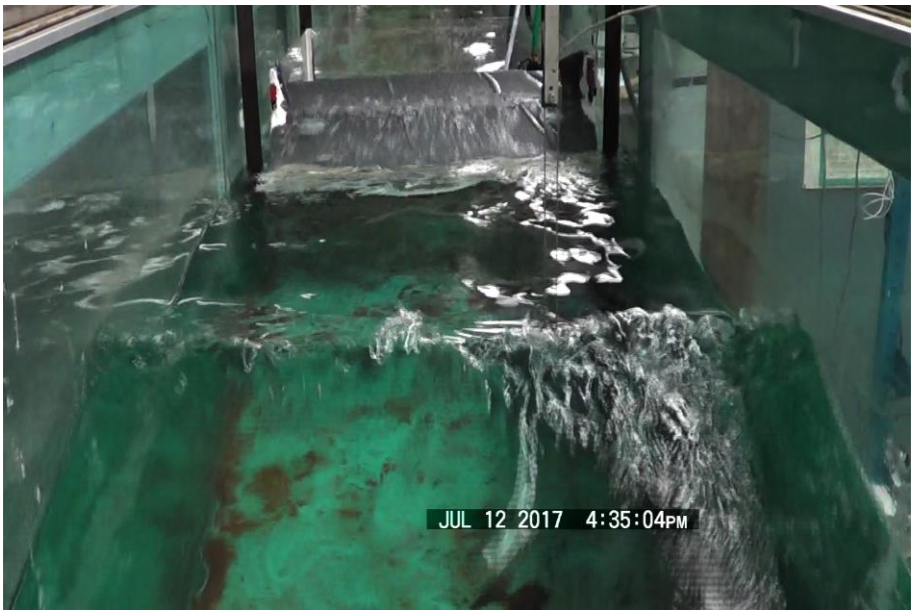

Figure 36. Wave Breaks in front of the Device

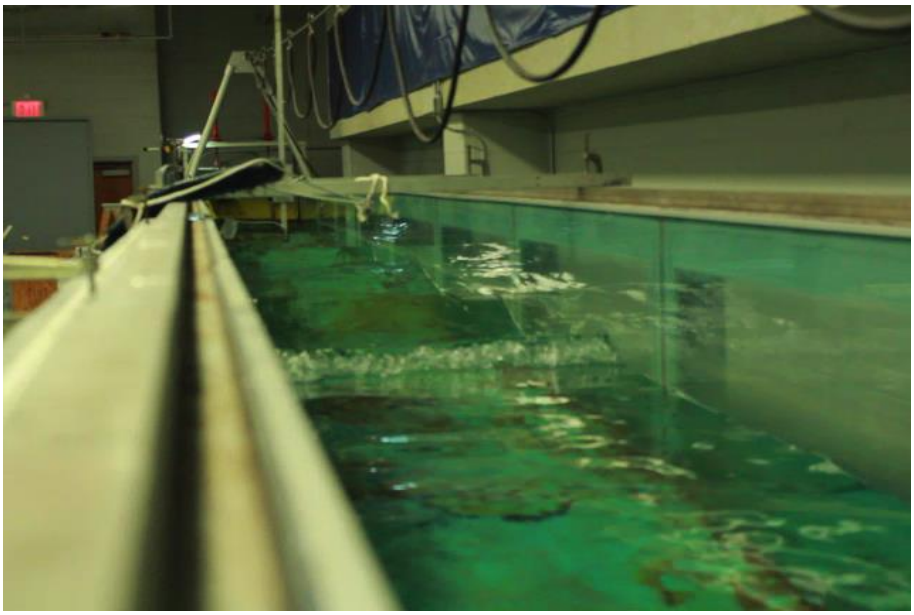

Figure 37. Wave Breaks far from the Device

Even though the result does not completely match with the results from others' studies, the trend of the result is consistent with the general formulae in Section 2.4. Thus, the fixed condition is reliable so that the next section will use this result to compare and determine that whether the application of the SMA spring is reasonable or not.

5.2 Adjustable Crest Freeboard Height

As mentioned in Section 4.1.4, it is hard to put a wave gauge far away from the device to detect the properties of the incoming waves. The alternative method is to test the overtopping discharge rate at different R_c at every wave condition. The result of this section is expected to follow the result of the fixed R_c condition. Therefore, in this section, the SMA springs are powered on and nine different temperatures have been chosen which

means that there will be nine different R_c, which are 0.068m (30℃), 0.071m (35℃), 0.078m (40℃), 0.090m (47.5℃), 0.096m (55℃), 0.102m (45℃), 0.103m (50℃), 0.111m (60℃), and 0.116m (65℃). From Figure 38 to Figure 42 show that all the night conditions. Figure 43 shows the R_c versus the temperature.

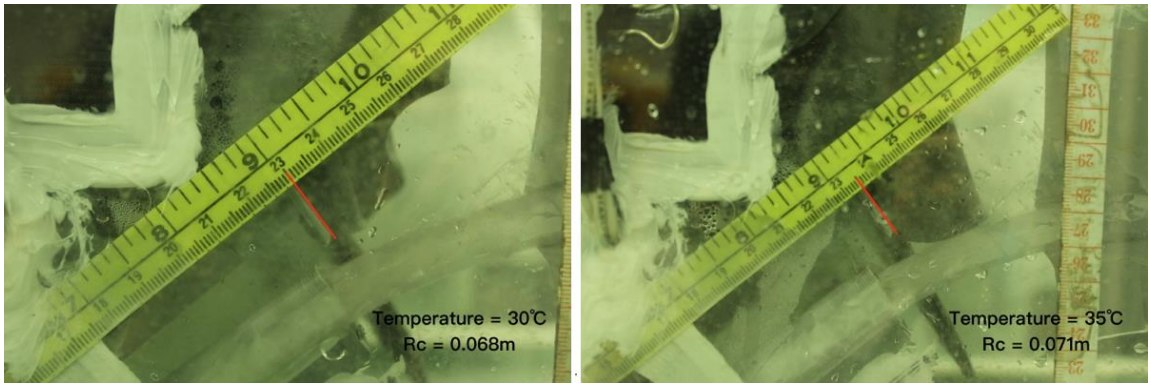

Figure 38. R_c = 0.068m for 30℃(Left), R_c = 0.071m for 35℃(Right)

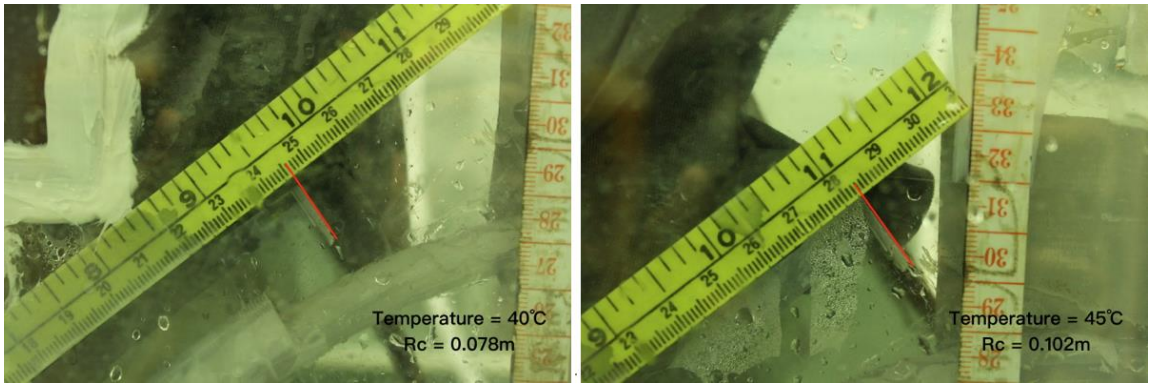

Figure 39. R_c = 0.078m for 40℃(Left), R_c = 0.102m for 45℃(Right)

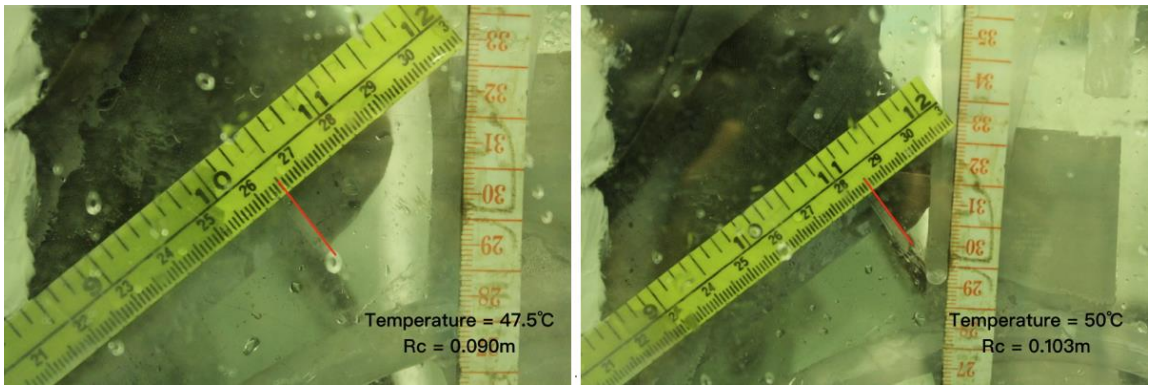

Figure 40. R_c = 0.090m for 47.5℃(Left), R_c = 0.103m for 50℃(Right)

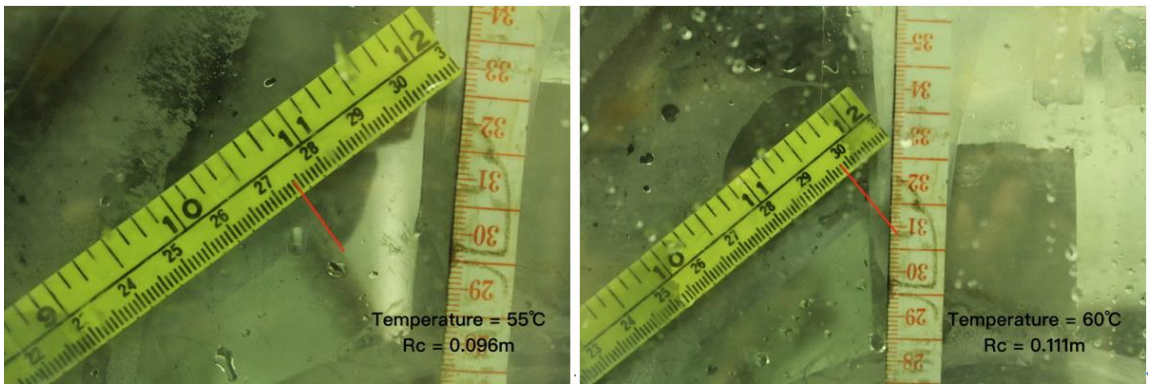

Figure 41. R_c = 0.096m for 55℃(Left), R_c = 0.111m for 60℃(Right)

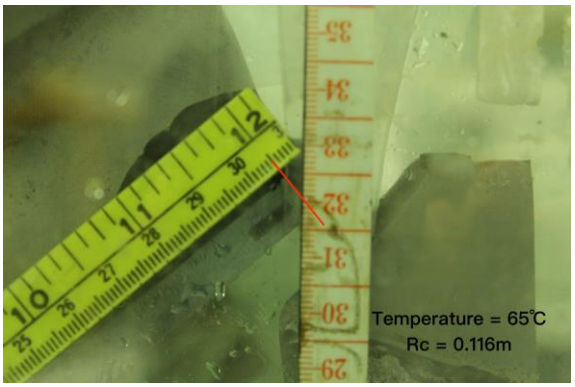

Figure 42. R_c = 0.116m for 65℃

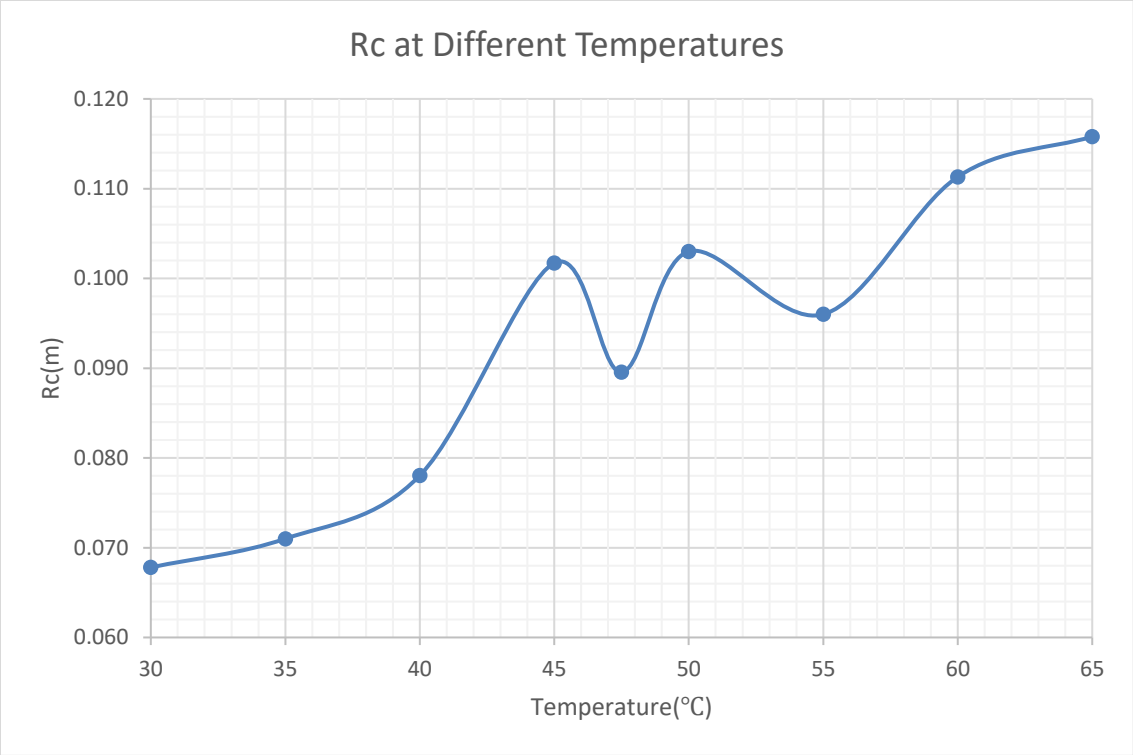

Figure 43. R_c at Different Temperatures

In Figure 43, the line shows that it is not smooth when the temperature comes to around 45℃. This is caused by the transition temperature of the SMA which means that a small difference of the temperatures will cause a different result in this region. Also, the setup and the condition of the device affect the data. The friction force on the rail varies from time to time and location to location. The factors that affect the friction force contain the room temperature, the humidity, the lubricant, and etc. If the installation of the rails can be improved to a perfect state, the relation between the R_c and the temperature can be more reasonable and consistent. However, the objective of the present thesis is to guarantee that the SMA can be applied on the OWEC and the feasibility of changing the

R_c without violating the rule of the overtopping phenomenon. Figure 44 shows the result of the adjustable condition. The result also follows an exponential line.

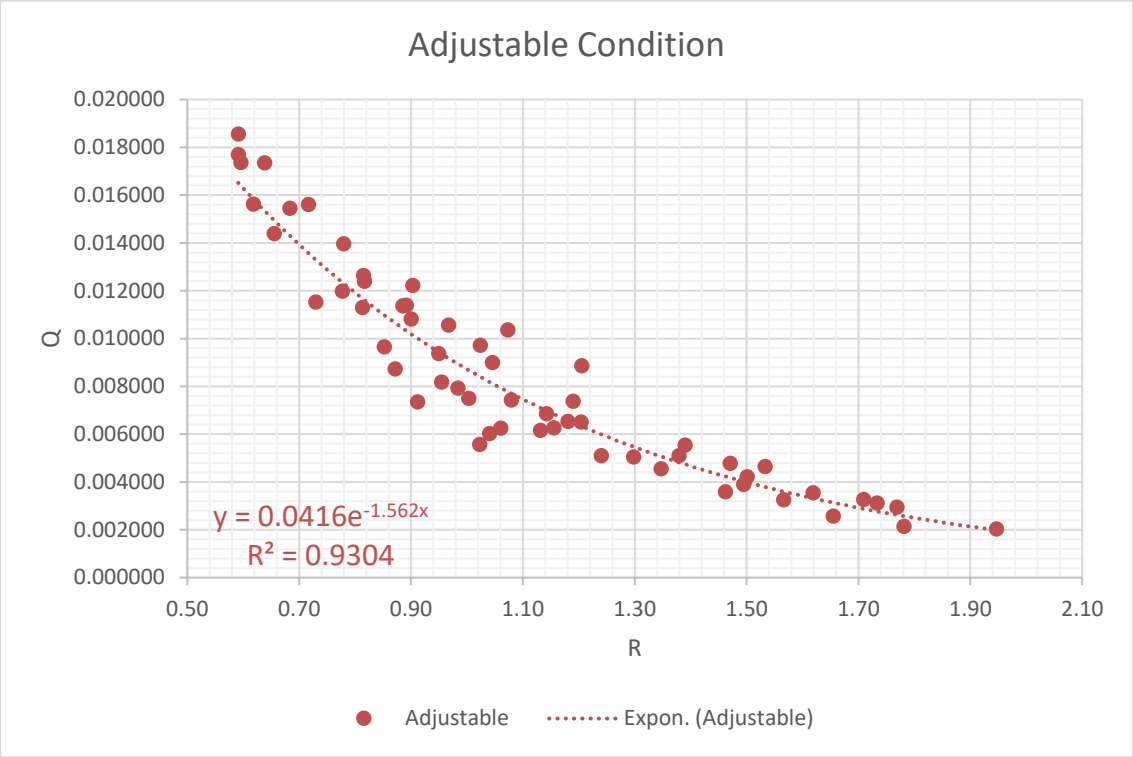

Figure 44. Adjustable Condition

In order to check whether the application of the SMA affect the result of the fixed condition or not, the experiment result of the adjustable condition is compared with the fixed condition which also fits into another exponential line. Figure 45 shows that all of the 58 adjustable experiment points surround the exponential line of the fixed condition. Some of them are a little away from the line so that another kind of comparison should be done to justify the feasibility.

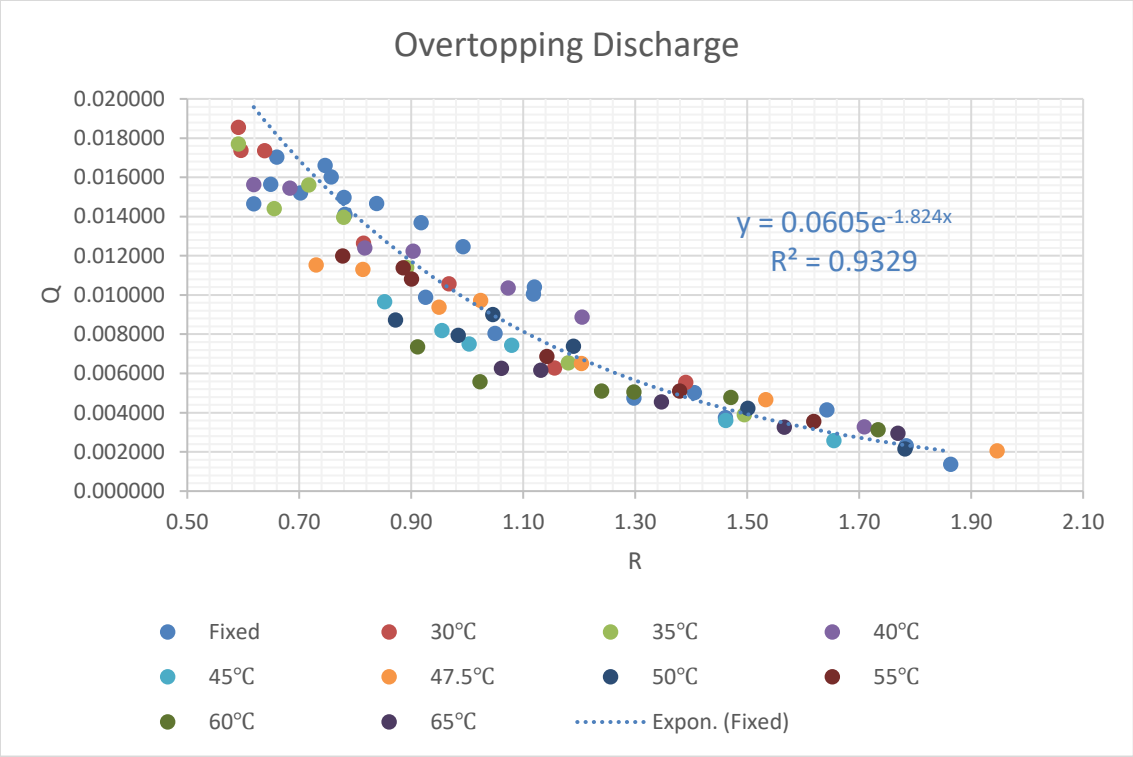

Figure 45. Adjustable Condition Data Points Surround the Fix Condition

In order to compare the difference between the fixed and the adjustable condition, the exponential lines of the adjustable condition and the fixed condition are compared and the errors are calculated. Figure 42 shows that two lines of two different conditions are close to each other which means that the application of the SMA spring will not affect the trend of the overtopping discharge.

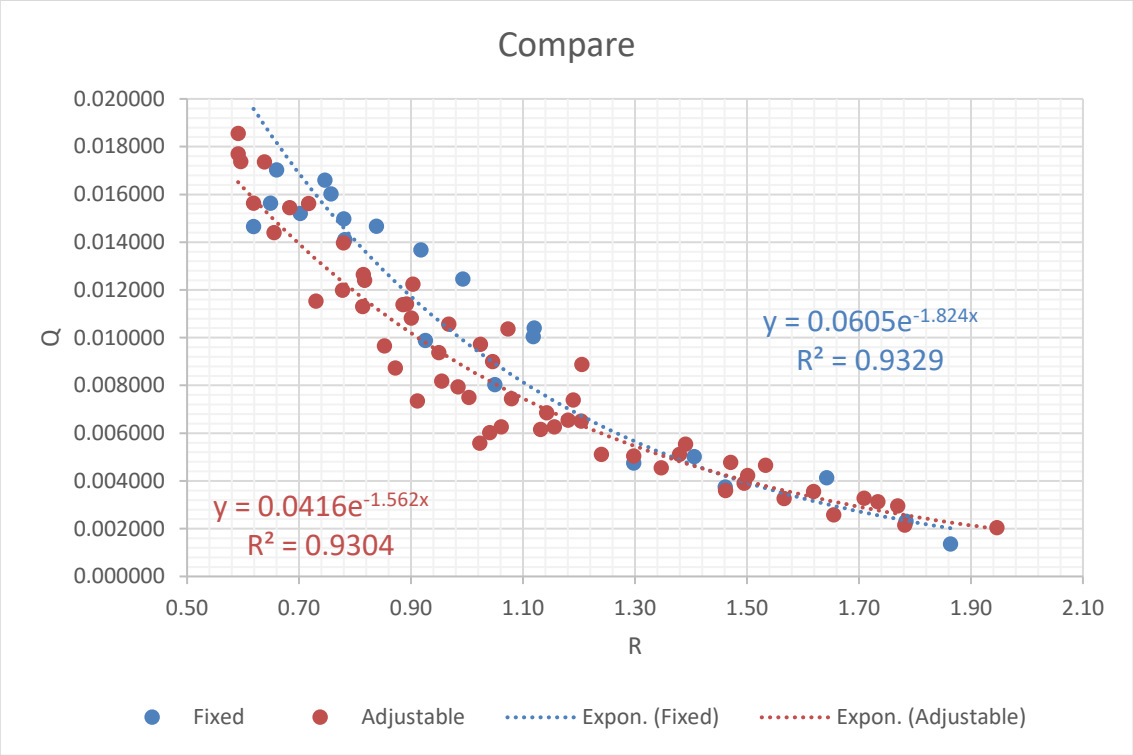

Figure 46. Comparison the Exponential Formulae of Two Conditions

In Figure 47, most of the error with the fixed exponential line lay in $\pm 20\%$ and the Table 3 shows that the average of error is -6.70% and the standard error is 2.36%. Both of them are acceptable while the overtopping phenomenon is dominated by the non-linearity. This means that the adjustable condition is pretty close to the fixed condition and the using of the SMA springs has no significant difference with one without it.

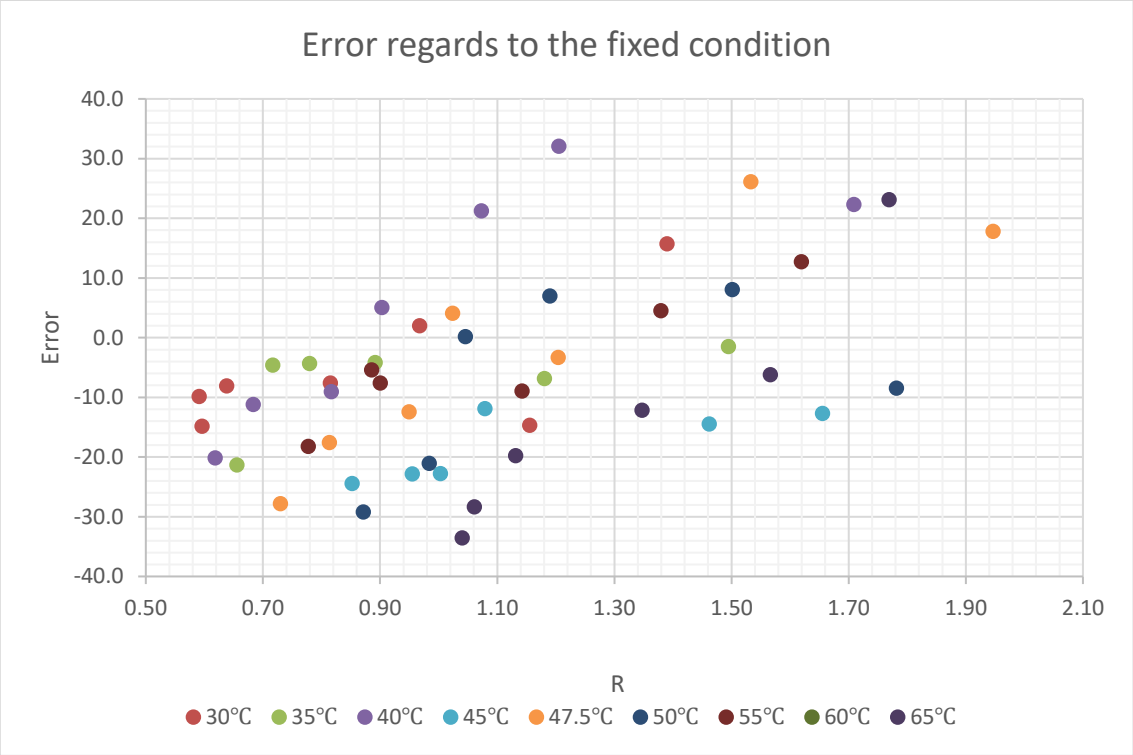

Figure 47. Error Compared with the Fixed Condition

Data Points	Average of Error (%)	Standard Error (%)
58	-6.70	2.36

Table 3. Average of Error and Standard Error

All these results indicate that the application of the SMA springs on the overtopping device is promising. The R_c can be adjusted to the desired value with different wave conditions. With proper R_c, the OWEC can be improved by either have more water being stored or more waves overtop.

6. CONCLUSIONS AND FUTURE WORK

6.1 Conclusions

This thesis represents a new concept to adapt to mutative wave conditions to obtain more wave power from the ocean. Therefore, the SMA springs are tested and installed on the OWEC model. The experiments only confirm the feasibility of the idea of using the SMA to change the crest freeboard height. The results have been divided into two parts, one without SMA springs and one with SMA springs. The result without SMA springs is compared with other's result and the general overtopping discharge formulae for OWECs. The comparison shows that the different experimental setup and the limitation of the water tank will cause the different overtopping discharge rate, but the tendency of the overtopping discharge rate is reasonable.

For the result of the application of the SMA springs, the result of non-using the SMA springs, the fixed condition, is regarded as the reference. The result shows that the installation of the SMA springs doesn't influence the trend of the overtopping discharge rate which is an exponential function. The comparison with the fixed condition also shows that there is no significant difference and the error which is caused by the nonlinearity of the overtopping phenomenon is acceptable. The concept of using the SMA to fit the different wave conditions is proven, but still have some issues need to be investigated and overcome in the future.

6.2 Future Work

Although the feasibility of the installation of SMA on the OWEC is proven, there are still some limitations need to be further considered. From the calibration of the SMA springs, the lack of consistency of the spring is shown. If the concept is going to be used in the prototype, the crest freeboard height should be more predictable so that the consistency of the function of the SMA springs should be taken into account. It can combine with other mechanical devices which make the SMA easier to keep the property in a stable state in a mutative environment.

Eventually, the concept of synchronizing the data of the upcoming waves with the control of the crest freeboard height with the SMA springs need to be applied. The goal is that a detecting system can calculate wave conditions meters away from the OWEC device and send a feedback to the SMA control system to change the crest freeboard height immediately and have the maximum efficiency of harvesting the wave power. This idea should be proven in a larger water tank and in real sea.

REFERENCES

1. Johanasson, T., et al., *Renewable fuels and electricity for a growing world economy-defining and achieving the potential.* Renewable Energy–Sources of Fuels and Electricity. Johnasson, TB, Kelly, H., Reddy, AKN and Williams, RH (eds). Island Press, Washington DC, USA, 1993.
2. Höök, M. and X. Tang, *Depletion of fossil fuels and anthropogenic climate change—A review*. Energy Policy, 2013. **52**: p. 797-809.
3. Sabine, C.L. and R.A. Feely, *CLIMATE AND CLIMATE CHANGE | Carbon Dioxide*. 2015: p. 10-17.
4. Administrator, U.S.E.I. *Electricity in the United States*. 2008 May 10, 2017; Available from: https://www.eia.gov/energyexplained/index.cfm/index.cfm?page=electricity_in_the_united_states.
5. Joselin Herbert, G.M., et al., *A review of wind energy technologies.* Renewable and Sustainable Energy Reviews, 2007. **11**(6): p. 1117-1145.
6. Mekhilef, S., R. Saidur, and A. Safari, *A review on solar energy use in industries.* Renewable and Sustainable Energy Reviews, 2011. **15**(4): p. 1777-1790.
7. Saidur, R., et al., *A review on biomass as a fuel for boilers.* Renewable and Sustainable Energy Reviews, 2011. **15**(5): p. 2262-2289.
8. Thy, P. and B.M. Jenkins, *Mercury in Biomass Feedstock and Combustion Residuals.* Water, Air, & Soil Pollution, 2009. **209**(1-4): p. 429-437.

9. Administrator, U.S.E.I. *Geothermal Energy*. 2008 November 8, 2016; Available from: https://www.eia.gov/energyexplained/index.cfm/index.cfm?page=geothermal_home.

10. Sánchez-Zapata, J.A., et al., *Effects of Renewable Energy Production and Infrastructure on Wildlife*. 2016. **1**: p. 97-123.

11. Administrator, U.S.E.I. *Tidal Power*. 2008 March 22, 2017; Available from: https://www.eia.gov/energyexplained/index.cfm/index.cfm?page=hydropower_tidal.

12. Administrator, U.S.E.I. *Ocean Thermal Energy Conversion*. 2008 September 22, 2017; Available from: https://www.eia.gov/energyexplained/index.cfm/index.cfm?page=hydropower_ocean_thermal_energy_conversion.

13. Administrator, U.S.E.I. *Wave Power*. 2008 January 10, 2017; Available from: https://www.eia.gov/energyexplained/index.cfm/index.cfm?page=hydropower_wave.

14. Day, A., et al., *Hydrodynamic modelling of marine renewable energy devices: A state of the art review*. Ocean Engineering, 2015. **108**: p. 46-69.

15. Pérez-Collazo, C., D. Greaves, and G. Iglesias, *A review of combined wave and offshore wind energy*. Renewable and Sustainable Energy Reviews, 2015. **42**: p. 141-153.

16. Falcão, A.F.d.O., *Wave energy utilization: A review of the technologies.* Renewable and Sustainable Energy Reviews, 2010. **14**(3): p. 899-918.

17. Rusu, E., *Evaluation of the Wave Energy Conversion Efficiency in Various Coastal Environments.* Energies, 2014. **7**(6): p. 4002-4018.

18. Frigaarda, P., et al., *3 years experience with energy production on the Nissum Bredning Wave Dragon Proto Type.* 2006.

19. Tedd, J., *Testing, analysis and control of the wave dragon wave energy converter*. 2007, Aalborg University, Department of Civil Engineering.

20. Jani, J.M., et al., *A review of shape memory alloy research, applications and opportunities.* Materials & Design, 2014. **56**: p. 1078-1113.

21. DYNALLOY, I. *FLEXINOL® Actuator Spring Technical and Design Data*. 2017; Available from: http://www.dynalloy.com/tech_data_springs.php.

22. Zhang, C., R.H. Zee, and P.E. Thoma. *Development of Ni-Ti based shape memory alloys for actuation and control*. in *Energy Conversion Engineering Conference, 1996. IECEC 96., Proceedings of the 31st Intersociety*. 1996. IEEE.

23. Strittmatter, J. and P. Gümpel, *Long-Time Stability of Ni-Ti-Shape Memory Alloys for Automotive Safety Systems.* Journal of Materials Engineering and Performance, 2011. **20**(4-5): p. 506-510.

24. Stoutenburg, E. *Combining Offshore Wind and Wave Energy Farms to Facilitate Grid Integration of Variable Renewables*. 2012 April 23, 2012; Available from: https://energy.stanford.edu/events/combining-offshore-wind-and-wave-energy-farms-facilitate-grid-integration-variable-renewables.

25. Wan, L., et al., *Comparative experimental study of the survivability of a combined wind and wave energy converter in two testing facilities.* Ocean Engineering, 2016. **111**: p. 82-94.

26. Martinelli, L. and P. Frigaard, *The Wave Dragon: tests on a modified model*. 1999: p. 30.

27. van der Meer, J.W. and J.P. Janssen, *Wave run-up and wave overtopping at dikes and revetments.* Delft Hydraulics, 1994.

28. Van der Meer, J., *Technical report wave run-up and wave overtopping at dikes.* TAW report (incorporated in the EurOtop manual), 2002.

29. Weggel, J.R., *Wave overtopping equation*, in *Coastal Engineering 1976*. 1977. p. 2737-2755.

30. *Manual on the use of rock in coastal and shoreline engineering*. CIRIA special publication: 83. 1991: Rotterdam ; Brookfield, VT : A.A. Balkema, 1991.

31. Parmeggiani, S., J. Kofoed, and E. Friis-Madsen, *Experimental Update of the Overtopping Model Used for the Wave Dragon Wave Energy Converter.* Energies, 2013. **6**(4): p. 1961-1992.

32. Juhl, J. and P. Sloth, *Wave overtopping of breakwaters under oblique waves*, in *Coastal Engineering 1994*. 1995. p. 1182-1196.

33. Sakakiyama, T. and R. Kajima, *Wave overtopping and stability of armor units under multidirectional waves*, in *Coastal Engineering 1996*. 1997. p. 1862-1875.

34. Kofoed, J.P., *Wave Overtopping of Marine Structures: utilization of wave energy*. 2002, Videnbasen for Aalborg UniversitetVBN, Aalborg UniversitetAalborg

University, Det Teknisk-Naturvidenskabelige FakultetThe Faculty of Engineering and Science, Institut for Vand, Jord og MiljøteknikDepartment of Civil Engineering.

35. Hasselmann, K., *Measurements of wind wave growth and swell decay during the Joint North Sea Wave Project (JONSWAP).* Dtsch. Hydrogr. Z., 1973. **8**: p. 95.

36. Schüttrumpf, H., et al., *Effects of natural sea states on wave overtopping of seadikes*, in *Ocean Wave Measurement and Analysis (2001)*. 2002. p. 1565-1574.

37. Ward, D.L., et al., *Wind effects on runup and overtopping of coastal structures*, in *Coastal Engineering 1996*. 1997. p. 2206-2215.

38. Gonzalez-Escriva, J., et al. *Wind effects on run-up and overtopping: influence on breakwater crest design*. in *Proceedings of the 28th International Conference Coastal Engineering-Solving Coastal Conundrums-Vol. 2*. 2003. World Scientific.

39. Wolters, G. and M.R. van Gent. *Maximum wind effect on wave overtopping of sloped coastal structures with crest elements*. in *Proc. Coastal Structures*. 2007.

40. Owen, M., *Design of seawalls allowing for wave overtopping.* Report Ex, 1980. **924**: p. 39.

41. Shankar, N. and M. Jayaratne, *Wave run-up and overtopping on smooth and rough slopes of coastal structures.* Ocean Engineering, 2003. **30**(2): p. 221-238.

42. Bruce, T., et al., *Overtopping performance of different armour units for rubble mound breakwaters.* Coastal Engineering, 2009. **56**(2): p. 166-179.

43. Hebsgaard, M., P. Sloth, and J. Juhl, *Wave overtopping of rubble mound breakwaters*, in *Coastal Engineering 1998*. 1999. p. 2235-2248.

44. Verwaest, T., et al., *Waves overtopping a wide-crested dike.* Coastal Engineering Proceedings, 2011. **1**(32): p. 7.

45. Grantham, K.N., *A Model Study of Wave Run-up on Sloping Structures*. 1953: University of California, Institute of Engineering Research.

46. Battjes, J.A., *Golfoploop en golfoverslag*. 1972, Rijkswaterstaat, DWW.

47. Victor, L. and P. Troch, *Wave overtopping at smooth impermeable steep slopes with low crest freeboards.* Journal of Waterway, Port, Coastal, and Ocean Engineering, 2012. **138**(5): p. 372-385.

48. Nielsen, A. and J.P. Kofoed, *The Wave Dragon: evaluation of a wave energy converter*. 1997.

49. Borgarino, B., J.P. Kofoed, and J. Tedd, *Experimental Overtopping Investigation for the Wave Dragon: effects of reflectors and their attachments.* 2007.

50. Victor, L., P. Troch, and J.P. Kofoed, *On the Effects of Geometry Control on the Performance of Overtopping Wave Energy Converters.* Energies, 2011. **4**(12): p. 1574-1600.

51. Liu, P.L.-F., et al., *Numerical modeling of wave interaction with porous structures.* Journal of waterway, port, coastal, and ocean engineering, 1999. **125**(6): p. 322-330.